

# Preparation, characterization, and bioactivities of polysaccharides fractions from sugarcane leaves

Mengmiao MO<sup>1</sup>, Fengyu JIANG<sup>1</sup>, Weiming CHEN<sup>1</sup>, Zhendong DING<sup>1</sup>, Yongguang BI<sup>1</sup>, Fansheng KONG<sup>1\*</sup> 

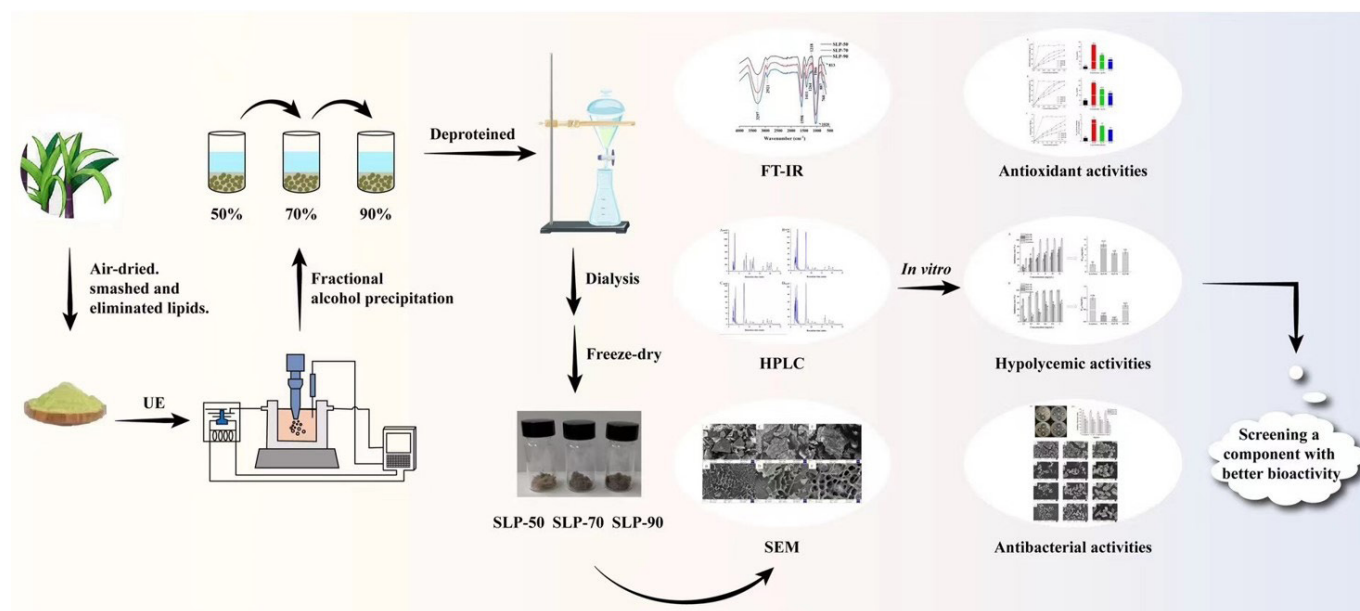
## Abstract

Three new polysaccharides (SLP-50, SLP-70, and SLP-90) were fractionated successively by gradient concentrations of ethanol. This study aimed to investigate the initial structural characterization and bioactivities of these sugarcane leaves polysaccharides (SLPs) obtained by ultrasound-assisted extraction. The results, which were further validated by IR spectrometry, revealed that the three SLPs contained uronic acids, proteins, and sulfate groups in addition to carbohydrate. SLP-50 (36.40 kDa), SLP-70 (12.97 kDa), and SLP-90 (3.52 kDa) were acidic heteropolysaccharides mainly comprised of mannose (Man), rhamnose (Rha), glucuronic acid (Glc A), galacturonic acid (Gal A), galactose (Gal), glucose (Glc), xylose (Xyl), and arabinose (Ara), in different molar ratios. SLP-90 exhibited higher antioxidant capacity than SLP-50 and SLP-70. *In vitro*, all fractions showed significant hypoglycemic potential and antibacterial activity against Gram-positive and Gram-negative bacteria. The IC<sub>50</sub> values of SLP-50, SLP-70, and SLP-90 were 0.11, 0.05, and 0.67 mg/mL on  $\alpha$ -glucosidase, respectively, which were significantly lower than that of acarbose (0.80 mg/mL). These findings could provide a reference for developing and applying SLP-based functional foods.

**Keywords:** sugarcane leaves polysaccharides; ultrasonic-assisted extraction; antioxidant effect; hypoglycemic effect; antibacterial activity

**Practical Application:** Ultrasonic-assisted extraction-alcohol precipitation process could be served as a promising preparation technology for the extraction of active polysaccharides from sugarcane leaves.

## Graphical Abstract



## 1 Introduction

*Saccharum officinarum* L., commonly known as sugarcane, is a species of *Saccharum* in the family *Poaceae*. It has been cultivated globally for hundreds of years for its high economic

value and nutrient richness and is one of the most widely grown crops in the world (Ali et al., 2021). As an abundant and healthy green resource, sugarcane leaves are highly valued in China due

Received 02 Sept., 2022

Accepted 23 Oct., 2022

<sup>1</sup>School of Pharmacy, Guangdong Pharmaceutical University, Guangzhou, China

\*Corresponding author: [fskongtx@163.com](mailto:fskongtx@163.com)

to their wide range of biological activities (Gui et al., 2012). They have been reported to have a remarkable protective effect against myocardial infarction, promoting myocardial repair and new blood vessel formation around the infarcted area and reducing the content of cTnI in serum (He et al., 2016). It is worth noting that polysaccharides are the primary components that protect cardiomyocytes. As one of the most important active components of sugarcane leaves, polysaccharides have a variety of health-promoting effects, such as antioxidant (Gui et al., 2012), antitumor (Zhong et al., 2012), antibacterial (Hou et al., 2010), hypoglycemic (Hou et al., 2011), and anti-inflammatory (Zhong et al., 2012) activities, which have been gradually discovered with the continuing breakthroughs in sugarcane research. Therefore, SLPs are likely to have high potential application value in the pharmaceutical and food industries.

The extraction process is the key to the use of natural polysaccharides in functional foods and pharmaceutical industries, and has a great influence on the yield, physicochemical properties and biological activities of natural polysaccharides (Fu et al., 2020). The conventional extraction methods for polysaccharides are time-consuming and inefficient, and the boiling-water extraction, acid/base leaching, etc., of some processes can degrade active ingredients (Liu & Huang, 2019). Ultrasonic extraction is a highly efficient emerging technology characterized by safety, minimal pollution, high extraction rate and low cost; and it has been widely used to extract active polysaccharides from plants (Chen et al., 2022). Ultrasound can greatly facilitate the extraction process by creating a cavitation effect that disrupts the cell walls, reduces particle size, and enhances contact between the solvent and the target compound. The mass transfer between the solution and the cells is enhanced, thereby saving time and energy (Chen et al., 2022; Wang et al., 2019a). Ultrasound has been proven to optimize the physical and chemical properties of food, and improve its functionality (Tang et al., 2016). Large polysaccharides with high molecular weight cannot easily cross cell membranes to enable their bioactive effects and have poor solubility and bioavailability (Yao et al., 2022). Therefore, it is necessary to break down the complex polysaccharides to increase their solubility and release the active moieties locked in the molecules for useful applications. As a physical degradation method, ultrasonic waves can break down polysaccharides and enhance their bioactive properties, such as antioxidant activity, by reducing the molecular weight without altering the basic structure (Surin et al., 2020). The purification method also strongly affects the physical/chemical properties and bioactivities of polysaccharides (Hui & Gao, 2022). Most plant-derived polysaccharides have a broad MW distribution, and complex heterogeneous polysaccharides may also have differences in the ratio of sugar components, types of linkage, branching arrangements, and degree of substitution (Jia et al., 2021). Hence, it is desirable to separate polysaccharides into fractions with different physicochemical properties and biological activities.

Ethanol precipitation is one of the most convenient and effective methods for the initial purification of polysaccharides because it is rapid, easy to perform, and effectively concentrates the molecules (Hui & Gao, 2022). The ethanol concentration has been shown to be the key factor in determining molecular size, structural characteristics and biological activities of polysaccharides

(Gu et al., 2020b). Jia et al. analyzed corn silk polysaccharide fractions separated by graded ethanol precipitation and found that these fractions had unique molecular weights, characteristic viscosities, particle sizes and microstructures (Jia et al., 2021; Chou et al., 2019). isolated three polysaccharides from *Pholiota nameko* by a fractional ethanol precipitation method, and reported that the polysaccharide fractions had totally different moisture retention properties and antioxidant potential, which indicated that ethanol fractional precipitation was an efficient method for obtaining polysaccharide fractions with different physicochemical characteristics and biological activities. However, to the best of our knowledge, no one has combined ultrasonic extraction with graded alcohol precipitation to obtain polysaccharide fractions for studying the relationship between physical/chemical properties and bioactivities of sugarcane leaves polysaccharide fractions (SLPs). Therefore, it is meaningful to investigate and compare the physicochemical properties and biological activities of SLPs using an ultrasound- fractionated precipitation technique.

In this study, three new active polysaccharides (SLP-50, SLP-70, SLP-90) were prepared by ultrasound-graded precipitation technology, and their chemical composition and monosaccharide types were determined by various techniques. HPLC, HPGPC, FT-IR, UV, NMR, TGA, and SEM were used to characterize the structure of the polysaccharides. In addition, the antioxidant, hypoglycemic and antibacterial effects of the fractions were compared. The relationships between the physical /chemical properties and the biological activities of the three fractions was systematically analyzed. This study provides important insights for the future exploration of the practical applications of sugarcane leaves polysaccharides in the food and pharmaceutical industries.

## 2 Materials and methods

### 2.1 Materials and reagents

Sugarcane leaves were acquired from a sales department at Gula Town, Binyang County, Nanning City. ABTS was provided by Macklin Biochemical Co., Ltd of Shanghai, China. DPPH was provided by Aladdin Biochemical Technology Co., Ltd of Shanghai, China. The *p*-nitrophenyl- $\alpha$ -D-glucopyranoside (PNPG),  $\alpha$ -glucosidase, and  $\alpha$ -amylase were obtained from Sigma Chemical Co., Ltd. (St. Louis, MO, USA). All reagents were of analytical grade.

The four microbial strains, *Salmonella typhimurium* (CMCC 50094), *Escherichia coli* (CMCC 44102), *Staphylococcus aureus* (CMCC 26003), and *Pseudomonas aeruginosa* (CMCC 10104) were obtained from the Guangdong Institute of Microbiology.

### 2.2 Extraction and separation of polysaccharides

The SLPs were extracted based on a previous method with necessary modifications (Li et al., 2017b). Fresh sugarcane leaves (1.0 kg) were dried, chopped, crushed, and passed through a 60-mesh sieve. The sieved material was processed with petroleum ether for 5 h and then pretreated twice with 95% ethanol, followed by drying at 60 °C for 48 h. The pre-treated powder was steeped in deionized water at a liquid/solid ratio of 40 mL/g for 3 h, then the mixture was sonicated two times for 1 h each time at 60 °C with an ultrasonic device at 360 W power. After filtration, the

filtrate (crude extract) was concentrated to 500 mL on a rotary evaporator at 55 °C. The concentrated aqueous solution was cooled to room temperature, then different quantities of absolute ethanol were added to obtain an increasing range of concentrations (50%, 70%, and 90%, v/v) successively, and kept at 4 °C overnight. After centrifuging for 15 minutes at 4500 rpm, the precipitates were dissolved in hot water and deproteinized using Sevag's reagent (chloroform: n-butanol = 4:1, v/v). The deproteinized solutions were dialyzed for 48 h using a 3500 Da bag, and the SLP-50, SLP-70, and SLP-90 fractions were freeze-dried (Figure 1).

### 2.3 Analysis of physical and chemical characteristics of SLPs

#### Chemical composition of SLPs

The sulfate, uronic acid, protein, and total phenolics content of SLPs were determined using the barium chloride-gelatin method (Fakhfakh et al., 2017), the m-hydroxy biphenyl method (Jiang et al., 2020), the Coomassie brilliant blue method (Chen et al., 2019a), and the Folin-Ciocalteu method (Yalcinkaya et al., 2022), respectively. The total sugar content was measured by the phenol-sulfuric acid procedure with glucose as standard (Wang et al., 2021b).

#### Determination of monosaccharide compositions

The PMP-pre-column HPLC method (Huang et al., 2015) was adopted to determine the monosaccharide compositions of the SLPs. Briefly, 5.0 mg of SLP sample was hydrolyzed in 2 M trifluoroacetic acid at 120 °C for 4 h, and 100 µL of hydrolysate was derivatized with an equal volume of PMP (0.5 M) for 1h at 70 °C. The derivatized aqueous solution was extracted with equal volumes of chloroform until most of the excess PMP was removed. The PMP derivatives were then analyzed by HPLC on a ZORBAX Eclipse XDB-C18 column (5 µm, Ø 4.6 × 250 mm) with UV detection at 245 nm. The column was eluted with 82.0% phosphate-buffered saline (pH 6.8) and 18.0% acetonitrile (v/v) at 30°C with a flow rate of 1 mL/min.

#### Measurement of molecular weights (Mw) of SLPs

The molecular weights of the SLPs were determined using a published method with some modifications (Hua et al., 2014). The Mw of the SLPs was calculated by high-performance gel-permeation chromatography (HPGPC) with 0.02 M monopotassium phosphate as eluent at a flow rate of 0.5 mL/min. The column was calibrated at 35°C using the T-series of dextran standards

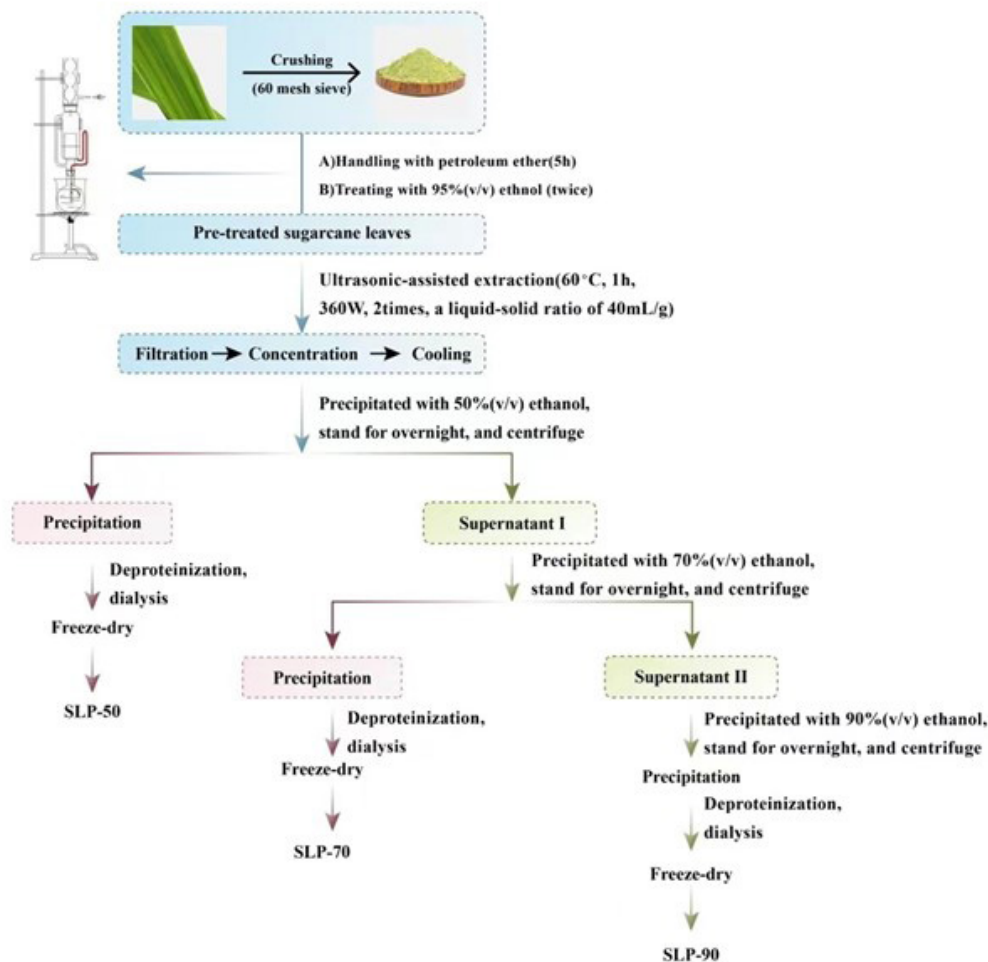


**Figure 1.** Flowchart for the extraction, separation, and fractionation of SLPs from sugarcane leaves.

with molecular weight at T1000, T500, T70, T40, T10, and T5. The Mw of each SLP was obtained from the regression equation.

#### Determination of zeta potential

The zeta potential of the polysaccharide solutions (1 mg/mL) was determined at 25°C using the Card Zeta potential/particle size analyzer (Delsa Nano C, USA). Each sample was replicated three times.

#### UV-vis spectra analysis

SLPs (0.5 mg/mL) were scanned by UV-vis spectrophotometer (UV-5500PC, Shanghai, China) in the 200-600 nm wavelength range.

#### FT-IR analysis

A KBr tablet method was utilized to scan the SLPs in the 4000-600  $\text{cm}^{-1}$  range using a Fourier-transform infrared spectrometer (PerkinElmer, USA).

#### NMR spectroscopy

SLP samples (60 mg) were dissolved in 0.6 mL  $\text{D}_2\text{O}$ , heated, sonicated, filtered through a 0.45  $\mu\text{m}$  filter after centrifugation, placed in an NMR tube, and analyzed with a Bruker 600 MHz nuclear magnetic resonance instrument (Rheinstetten, Germany) to obtain their  $^1\text{H}$  and  $^{13}\text{C}$  NMR spectra.

#### Thermogravimetric analysis (TGA)

The samples (~5 mg) were placed in an alumina pan, nitrogen was used as the heating medium, and the temperature went from 30°C to 600 °C at a heating rate of 20 °C/min (Zhou & Zhang, 2022).

#### Scanning electron microscope (SEM) analysis

The polysaccharide sample was placed on a metal platform and coated with a thin layer of gold. The samples were imaged using a SEM (SEM, Sigma 300, Zeiss, Germany) at 5.0 kV acceleration voltage and image magnification of 300× and 1000×.

### 2.4. Antioxidant activity of SLPs

#### Scavenging DPPH radical activity assay

The DPPH radical-scavenging activity was determined using a published technique (Yu et al., 2022), with minor modifications. In a test tube, 2 mL of the sample solution (0.02-0.12 mg/mL) was mixed with 2 mL of DPPH solution (0.1 mmol/L), vortexed, and reacted in the dark for 30 minutes, with the absorbance value recorded at 517 nm. Vc was taken as the positive control. The DPPH radical scavenging rate was calculated using the Formula 1 below:

$$\text{DPPH radical scavenging rate (\%)} = \left(1 - \frac{A_I - A_J}{A_0}\right) \times 100 \quad (1)$$

where  $A_I$ :denotes the absorbance of the sample;  $A_J$ :denotes the absorbance of the sample in the presence of ethanol;  $A_0$ :denotes the absorbance of the DPPH in the absence of the sample.

#### Assay for ABTS radical-scavenging

The ABTS radical-scavenging assay was accomplished using a published technique with some modifications (Hardinasinta et al., 2022). ABTS and potassium persulfate were dissolved in deionized water at 7 mM and 2.45 mM. Then the above solutions were evenly mixed in equal volumes, and the mixture (ABTS<sup>+</sup> solution) was diluted with ethanol until the absorbance value was  $0.70 \pm 0.02$  at 734 nm. Afterwards, 2.0 mL of the ABTS<sup>+</sup> solution was added to 0.2 mL of sample (0.04-0.24 mg/mL). The absorbance of the mixture was measured at 734 nm after 6 min of incubation at room temperature in the dark. Vc was used as positive control. The ABTS<sup>+</sup> scavenging rate was computed by the following Equation 2:

$$\text{ABTS}^{+} \text{ scavenging rate (\%)} = \left(1 - \frac{A_1 - A_2}{A_0}\right) \times 100 \quad (2)$$

Where  $A_1$  is the sample absorbance,  $A_2$  is the sample absorbance in the absence of ABTS<sup>+</sup>, and  $A_0$  is the absorbance of the ABTS<sup>+</sup> solution in the absence of the sample.

#### Assay of reducing power

The reducing power was measured following a previously reported method (Mitrović et al., 2022). The samples (1 mL) at various concentrations (1.0-3.5 mg/mL) were combined with 2.5 mL of 0.2 M PBS (pH 6.6) and 2.5 mL of  $\text{K}_3[\text{Fe}(\text{CN})_6]$  solution (1%, w/v). After the mixture had been incubated for 20 minutes at 50°C, 2.5 mL of 10% (w/v) trichloroacetic acid of was added. The mixture was then centrifuged for 10 minutes at 5000 rpm, and the supernatants (2.5 mL) were mixed with 0.5 mL of 0.1% (w/v)  $\text{FeCl}_3$  solution and 2.5 mL of distilled water. The absorbance at 700 nm ( $A_{700}$ ), which reflects the reducing power was measured after 10 minutes of reaction. Vc was taken as the positive control.

### 2.5. In vitro hypoglycemic activity

The hypoglycemic efficacy of the SLPs was determined *in vitro* by evaluating their inhibitory activities on  $\alpha$ -amylase and  $\alpha$ -glucosidase as previously described (Tang et al., 2021). A range of concentrations of SLPs (2.0-12.0 mg/mL) were tested in the assay for  $\alpha$ -amylase inhibition and serial dilutions of SLPs (0.1-1.0 mg/mL) in the assay for  $\alpha$ -glucosidase inhibition. Acarbose was used as positive control.

### 2.6. Antibacterial activity

#### Test organisms

The bacteriostatic activity of SLPs was evaluated against three Gram-negative bacteria: *Escherichia coli* (*E. coli*), *Salmonella typhimurium* (*S. typhimurium*), and *Pseudomonas aeruginosa* (*P. aeruginosa*). One Gram-positive bacterium, *Staphylococcus aureus* (*S. aureus*), was tested.

### Measurement of inhibition zone diameters

In this study, the paper disk diffusion method was employed to assess the antibacterial effects of the three SLPs (Zhang et al., 2020b). The test bacterial strains ( $1 \times 10^6$  CFU/mL) were diluted with sterile physiological saline, and 50  $\mu$ L of the diluted bacterial suspension was uniformly spread on Mueller-Hinton agar. Filter-paper discs (6 mm) were soaked in SLP solution for 2 h, then blotted and placed on the agar surface, and the plates were incubated 24 h at 37 °C. The diameter of the inhibitory zones was used as a measure of the antibacterial activity of SLPs. The positive control was levofloxacin (50  $\mu$ g/mL). All the measurements were carried out in triplicate. Antibacterial activity was categorized as weak (inhibition zone < 9 mm), weak to moderate (inhibition zone 9-15 mm), moderate (inhibition zone 15-19 mm), and high (inhibition zone  $\geq$  20 mm).

### Minimum inhibitory concentrations (MICs)

The MICs of SLPs were determined using a previous approach with minor modifications (Hajji et al., 2019). Briefly, Mueller-Hinton broth (MHB) was used to dilute the samples in a two-fold series of 0.039-10 mg/mL. Diluted samples (100  $\mu$ L) were mixed with 50  $\mu$ L of bacterial suspension ( $1 \times 10^5$  CFU/mL), then incubated at 37°C for 16 h. The MIC was defined as the sample concentration where the bacteria did not grow (by naked eye observation). Levofloxacin was taken as the positive control (50  $\mu$ g/mL).

### Effects of SLP on bacterial ultrastructure (SEM imaging)

The ultrastructure of bacteria was analyzed by SEM (Zhang et al., 2020b). *S. aureus* and *E. coli* were pretreated with an SLP sample (10 mg/mL) at 37°C for 6 h. The mixture was then centrifuged for 5 minutes at 8000 rpm. After removing the

supernatant, the bacterial cells were washed with 0.1 M PBS, and fixed in 1 mL of 4% glutaraldehyde (v/v) overnight at 4°C. After centrifugation, the fixed bacteria were washed three times with PBS and fixed for another 1 h in 1 mL of 2% glutaraldehyde (v/v) at 4°C. The bacteria were subjected to graded dehydration with 20%, 50%, 80%, and 100% ethanol, respectively. Afterwards, the ethanol was replaced by tert-butanol. Negative controls were untreated *S. aureus* and *E. coli*. After the bacteria were dried, the cells were gold-coated and imaged by SEM.

### 2.7 Statistical analysis

All the assays were carried out in triplicate and the data were given as mean  $\pm$  SD. After performing ANOVA, significance was set at  $p < 0.05$ . Origin Software 2018 and SPSS software version 26.0 were utilized for statistical analyses.

## 3 Results and discussion

### 3.1 Physical and chemical characteristics of SLPs

#### Analysis of chemical constituents and molecular weights

The yield and chemical composition of the polysaccharide fractions from sugarcane leaves are listed in Table 1. The yields increased in the order of SLP-50 < SLP-70 < SLP-90, which indicated that SLP-70 and SLP-90 were the main polysaccharides of sugarcane leaves. Proteins and uronic acid were detected in all fractions, indicating that SLPs were acidic glycoprotein compounds. Similar data were seen with soybean polysaccharides (Wang et al., 2019b), where SHSP20, SHSP40, and SHSP60 from soybean were found to be acidic glycoprotein compounds. The highest total sugar content ( $50.54\% \pm 1.01\%$ ) and sulfate radical ( $38.94\% \pm 1.09\%$ ) content, as well as the minimum amount of uronic acid ( $4.21\%$ ) and protein ( $1.07 \pm 0.05\%$ ) were measured in SLP-50.

**Table 1.** The yield and physicochemical properties of three fractions from sugarcane leaves by using different concentration ethanol.

| Index                              | Samples            |                    |                    |
|------------------------------------|--------------------|--------------------|--------------------|
|                                    | SLP-50             | SLP-70             | SLP-90             |
| Yield (w %)                        | 1.22 $\pm$ 0.16c   | 1.89 $\pm$ 0.05b   | 2.71 $\pm$ 0.08a   |
| Total sugar (w %)                  | 50.54 $\pm$ 1.01a  | 45.11 $\pm$ 1.02ab | 40.04 $\pm$ 0.02b  |
| Sulfuric radical (w %)             | 38.94 $\pm$ 1.09a  | 31.71 $\pm$ 0.02b  | 15.96 $\pm$ 0.04c  |
| Uronic acid (w %)                  | 4.21 $\pm$ 0.02b   | 4.96 $\pm$ 0.03b   | 7.35 $\pm$ 0.05a   |
| Protein (w %)                      | 1.07 $\pm$ 0.05b   | 3.32 $\pm$ 0.04a   | 3.35 $\pm$ 0.03a   |
| Total phenolics (w %)              | 4.21 $\pm$ 0.30b   | 7.91 $\pm$ 0.50a   | 8.23 $\pm$ 0.20a   |
| Zeta potential (mV)                | -19.60 $\pm$ 1.67a | -23.47 $\pm$ 1.89b | -27.13 $\pm$ 0.52c |
| Average molecular weight (kDa)     | 36.40              | 12.97              | 3.52               |
| Monosaccharide composition (mol %) |                    |                    |                    |
| Gal                                | 32.62              | 30.27              | 21.12              |
| Glc                                | 12.05              | 16.89              | 41.34              |
| Ara                                | 18.15              | 18.87              | 9.96               |
| Man                                | 17.05              | 13.11              | 8.31               |
| Rha                                | 6.70               | 5.62               | 7.41               |
| Xyl                                | 4.82               | 11.62              | 8.97               |
| GalA                               | 6.69               | 2.10               | 1.65               |
| GlcA                               | 1.92               | 1.51               | 1.25               |

Values are indicated as mean  $\pm$  SD (n = 3). Means are significantly different with the different letters in the same row ( $p < 0.05$ ).

The higher the molecular weight (Mw) of a polysaccharide, the longer the molecular chain (Gu et al., 2020a), which is one of the most important structural elements relating to the bioactivity of a polysaccharide (He et al., 2018). As indicated in Figure 2, SLP-50 possesses two narrow and unsymmetrical elution peaks, suggesting that it consists mainly of a high-Mw and a low-Mw component. Based on the peak area, the high-Mw component is predominant at 58.14%. The average molecular weight of SLP-50 was calculated to be 36.40 kDa. Both SLP-70 and SLP-90 had one main peak, wide and unsymmetrical, which indicated that they contained only a single component. Their average molecular weight was determined to be 12.97 kDa and 3.52 kDa, respectively. The molecular weights of the three polysaccharide fractions decreased sequentially in the order of SLP-50 (36.40 kDa) > SLP-70 (12.97 kDa) > SLP-90 (3.52 kDa). This trend could be attributed to the change in ethanol concentration. When ethanol is added to a polysaccharide solution, it begins to dehydrate the molecules because of the strengthening of intramolecular hydrogen bonds, followed by conformational transition and assembly (Gu et al., 2020b). The PDI of the three SLPs was >2, indicating that they all were polydisperse aggregates. The molecular weight of SLPs extracted with hot water (SLP-90A) by Hou et al. was 10.70 kDa (He et al., 2016), which is considerably higher than our SLP-

90 (3.52 kDa). Our results suggest that ultrasonic extraction could cause hydrolytic cleavage of polysaccharide chains and breakage of intermolecular hydrogen bonds. A portion of the high Mw component was converted into a low Mw component, thereby increasing the low Mw content. Other small peaks were observed in the SLP elution profiles, which were oligosaccharides. The above findings indicated that ultrasonic-assisted alcohol precipitation extraction with different concentrations of ethanol could have an impact on the distribution of polysaccharide components.

#### Analysis of monosaccharide compositions

HPLC is commonly used for qualitative and quantitative analysis of the monosaccharide composition of polysaccharides. As illustrated in Table 1 and Figure 3, a minor amount of GalA and GlcA were detected in the SLPs, and SLP-50 had the highest content of galacturonic acid (6.69%) compared to SLP-70 (2.10%) and SLP-90 (1.65%); the existence of these minor components might be ascribed to more complexity in the polysaccharide composition. For SLP-50 and SLP-70, Gal was identified as the main monosaccharide at 32.62% and 30.27%, respectively, while the major monosaccharide of SLP-90 was Glc at 41.34%. Compared to SLP-50 and SLP-70, the content of Gal (21.12%) in

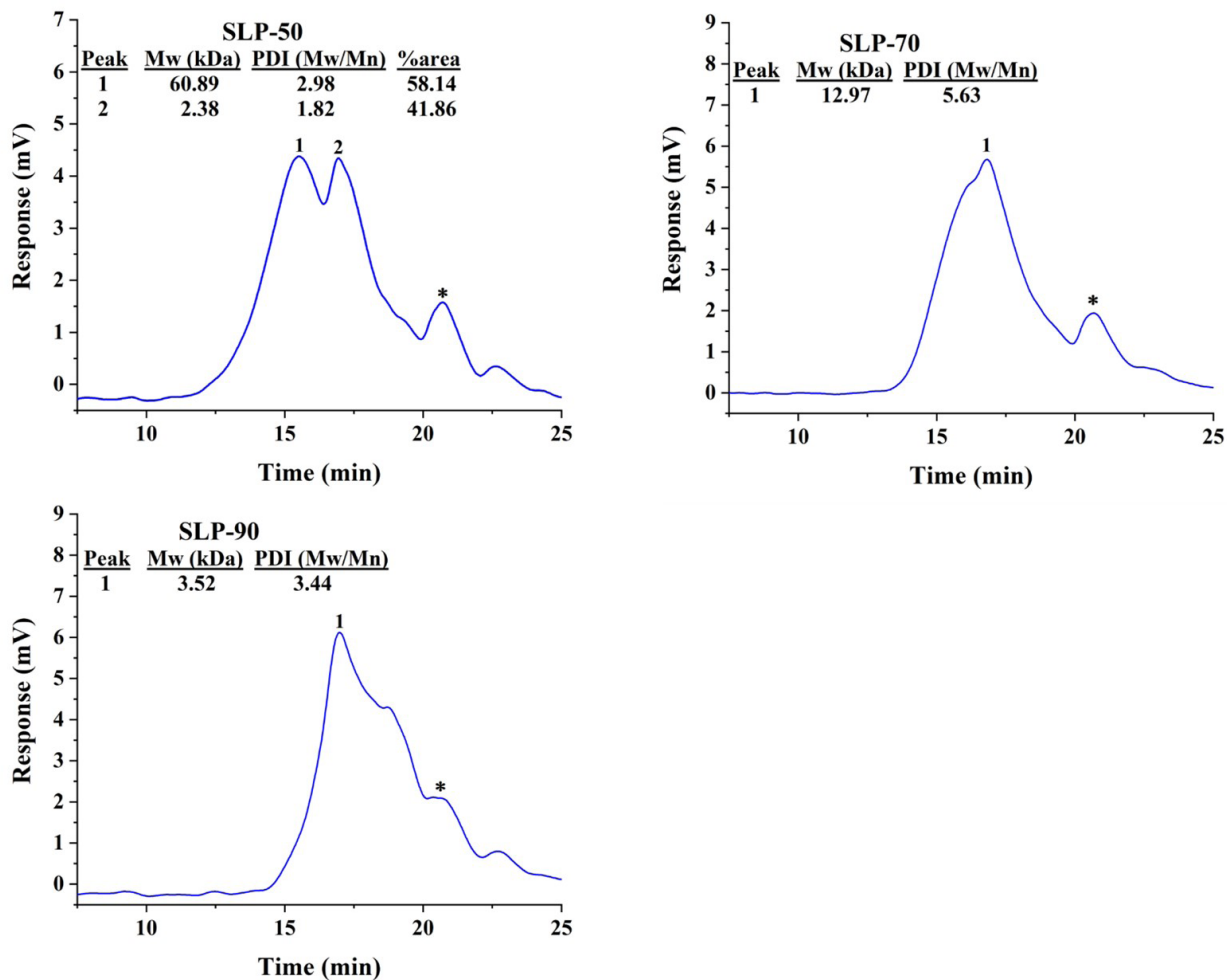


**Figure 2.** The molecular weight (Mw) distribution of various fractions of polysaccharides from sugarcane leaves, \* is regarded as an impurity.

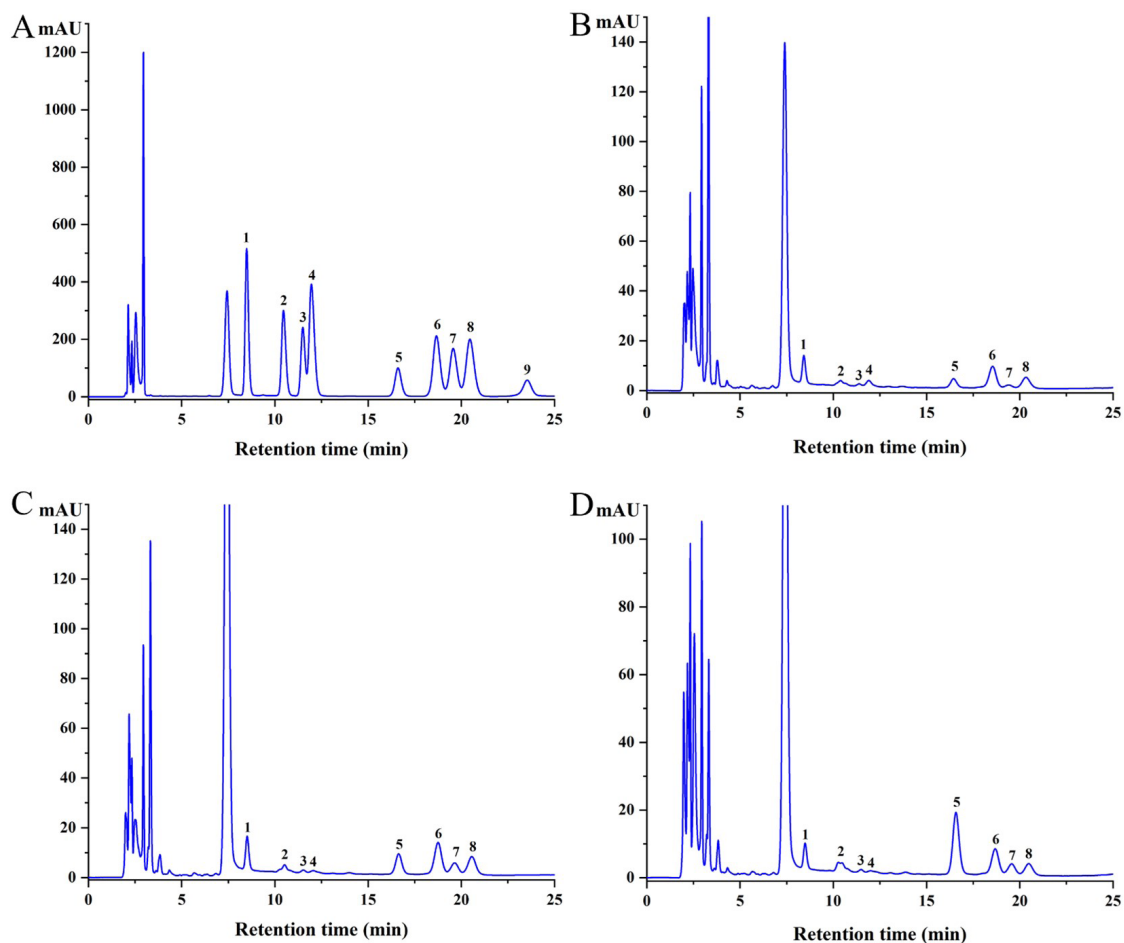


**Figure 3.** HPLC chromatograms of monosaccharides of SLPs. (A) Standard monosaccharides; peaks: (1) Man, (2) Rha, (3) GlcA, (4) GalA, (5) Glc, (6) Gal, (7) Xyl, (8) Ara, (9) Fuc; (B) SLP-50; (C) SLP-70; (D) SLP-90.

SLP-90 was significantly lower, while the amount of Glc (41.34%) was substantially increased, suggesting that SLP-90 might be a starch-like polysaccharide (Zhu et al., 2019). SLP-90 showed the highest Rha content, while the levels of Ara and Xyl were highest in SLP-70. Since all the polysaccharide fractions contained galactose, glucose, arabinose, mannose, rhamnose, xylose, galacturonic acid, and glucuronic acid, albeit in very different molar ratios, they were classified as acidic heteropolysaccharides with different monosaccharide compositions. Researchers found that polysaccharides extracted from sugarcane juice by the hot water method consisted of rhamnose, ribose, xylose, arabinose, mannose, galactose, and glucose in the ratio of 1:1.04:2.47:5.29:4.59:5.69:10.89 (Ban et al., 2013) (ribose was not measured in our study). The variations in monosaccharide composition might be attributed to differences in extraction and purification methods. Furthermore, the variety, source, and part of the sugarcane plant used for the extraction may also lead to differences in the monosaccharide composition.

#### Zeta potential

Zeta potential is defined as the magnitude of the electrostatic repulsion or attraction between particles. The charge properties

of polysaccharides can influence solution or colloid stability (Chen et al., 2019b). In general, the higher the absolute value of the zeta potential of a system of particles, the greater its stability (Gu et al., 2020a). The zeta potentials of the three polysaccharide fractions are shown in Table 1, with SLP-90 having the highest negative charge at  $-27.13 \pm 0.52$  mV. Uronic acids are the primary source of negative charge in polysaccharides (He et al., 2018), and this is consistent with our results in section 3.1.1 that SLP-90 possesses the highest uronic acid content. With the highest absolute value of negative charge, SLP-90 has better stability, which is conducive to the preparation of a stable mixed solution or colloid of SLP-90 (Chen et al., 2021b). This result was similar to those of the polysaccharides from the stem barks of *Acanthopanax leucorrhizus* (Hu et al., 2018).

#### UV-vis spectra and FT-IR analysis of SLPs

All three SLPs displayed a maximum absorption peak around 200 nm (Figure 4A), which is characteristic of polysaccharides (Li et al., 2017b). Weak absorption peaks around 280 nm indicated the presence of small amounts of proteins (He et al., 2015) (Table 1), but the absence of absorption at 260 nm confirmed that the SLPs did not contain nucleic acids (Li et al., 2017b).

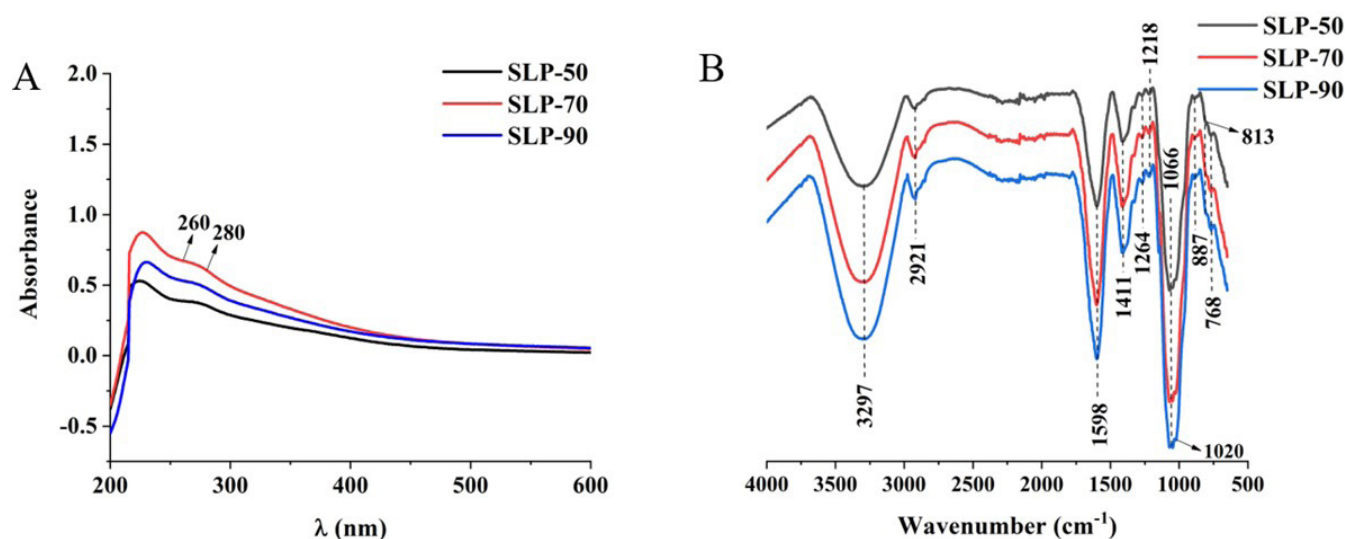


Figure 4. UV-vis spectra of polysaccharides from sugarcane leaves (A); FT-IR spectrum of SLPs (B).

These results demonstrate that the deproteinization method is very effective.

FT-IR spectrometry has been extensively used to characterize polysaccharides since it provides important information on functional groups in the chemical structure of polymers. The FT-IR spectrum was used to capture the typical characteristics of SLPs from 600  $\text{cm}^{-1}$  to 4000  $\text{cm}^{-1}$ . As can be seen in Figure 4B, the intensities of the peaks differed significantly in these polysaccharides. SLP-70 and SLP-90 had considerably higher absorption near 3297  $\text{cm}^{-1}$ , 2921  $\text{cm}^{-1}$ , 1598  $\text{cm}^{-1}$ , 1411  $\text{cm}^{-1}$ , and 1066  $\text{cm}^{-1}$  than SLP-50. An intense and wide absorption peak at about 3297  $\text{cm}^{-1}$  was assigned to the stretching vibration of -OH, and the faint signal near 2921  $\text{cm}^{-1}$  was attributed to the asymmetric stretching of the C-H bond in the sugar ring (Zhang et al., 2013). These two absorption bands were typical of the hydroxyl and alkyl functional groups of polysaccharides, respectively. For uronic acids, a strong band at 1598  $\text{cm}^{-1}$  corresponded to the asymmetric stretching of COO<sup>-</sup>, while another absorption band at 1411  $\text{cm}^{-1}$  was attributed to O-C-O binding (Vicente-García et al., 2004). All the samples had a stretching vibration peak at 1264  $\text{cm}^{-1}$  from the ester sulfate group (S=O) (Santhiya et al., 2002), which was the most prominent signal for the polysaccharides. Absorption peaks at 1218  $\text{cm}^{-1}$  and 1021 - 1082  $\text{cm}^{-1}$  indicated that the SLPs might contain pyranose sugar linked to the C-O-C or C-O-H stretching vibration (Yin et al., 2018). In addition, the absorption peaks at 813  $\text{cm}^{-1}$  come from the C-O-C vibration stretching in the furanose ring (Hou, 2014; Xie et al., 2022). The unique  $\beta$ -glycosidic linkage absorption peak at 887  $\text{cm}^{-1}$  implied the existence of  $\beta$ -glucans in the SLPs (Mathlouthi M Fau - Koenig & Koenig). Furthermore, the weak bands of ring deformation and ring stretching from  $\alpha$ -D-(1-6) and  $\alpha$ -D-(1-4) linkages were near 768  $\text{cm}^{-1}$  (Wang et al., 2019b), which was consistent with the results of polysaccharides from spent *Lentinus edodes* substrate (Wang et al., 2021a). According to these findings, we concluded that the SLP fractions were heteropolysaccharides composed of characteristic groups of hydroxyl, alkyl, ester,  $\beta$ -glucans, and D-pyran and furan rings.

#### NMR spectroscopy

Nuclear magnetic resonance is a highly useful tool for analyzing the structure of polysaccharides; it provides data on the sugar residues, glycosidic bonds, anomeric configurations, etc. The  $^1\text{H}$  NMR and  $^{13}\text{C}$  NMR spectra of SLPs are shown in Figure 5. In the  $^1\text{H}$  NMR spectrum, the presence of polysaccharides was confirmed by low-field resonances in a narrow region from  $\delta$ 3 to 6 ppm, and signals from anomeric hydrogens of polysaccharides were observed at 4-6 ppm, where most of the anomeric hydrogens in the 5-6 ppm range belong to the  $\alpha$  configuration. Most of the anomeric hydrogens in the 4-5 ppm range were in the  $\beta$  configuration, which confirmed that both  $\alpha$  and  $\beta$  configurations existed in SLPs, and the peaks observed in the anomeric region belonged to sugar residues. At  $\delta$ 3.67 ppm, the very strong signal is from the characteristic peak of the hydrogen in the methoxy group (-O-CH<sub>3</sub>). The methyl esterified carboxyl group (COO-CH<sub>3</sub>) of uronic acid appeared between 1.828 and 2.112 ppm, and the -CH<sub>3</sub> signal at 1.19 ppm belonged to rhamnose. For  $^{13}\text{C}$  NMR, the SLPs showed signals of anomeric carbons in the range of 92.23-109.43 ppm, revealing the existence of both  $\alpha$  ( $\delta$  95-101 ppm) and  $\beta$  ( $\delta$  95-101 ppm) anomeric configurations. This result is consistent with that of the  $^1\text{H}$  NMR spectrum. The chemical shift of the anomeric carbon was higher or lower than 107 ppm, indicating the presence of both furan and pyran rings in SLPs. We speculated that the carbon signal here belonged to  $\alpha$ -L-Ara, and the carbon signal around  $\delta$  99 ppm was assigned to  $\alpha$ -Glc, which may have multiple connection modes. The carbon signal in the  $\delta$  103 ppm range was assigned to  $\beta$ -gal, while the carbon signal at  $\delta$  92 ppm came from the small amount of  $\alpha$ -Xyl. A low-field signal at  $\delta$  170 ppm in the  $^{13}\text{C}$  NMR spectrum revealed the presence of uronic acids, and the carbon signal from  $\delta$ 55 to  $\delta$ 81 was attributed to residues C<sub>2</sub>-C<sub>6</sub>. In addition, some differences between them can be seen (Figure 5). The SLPs can have different intensities for the same signal peak. For example, compared to the other two polysaccharides, the signal peak near  $\delta$ 107 ppm of SLP-90 was so weak as to be almost absent.

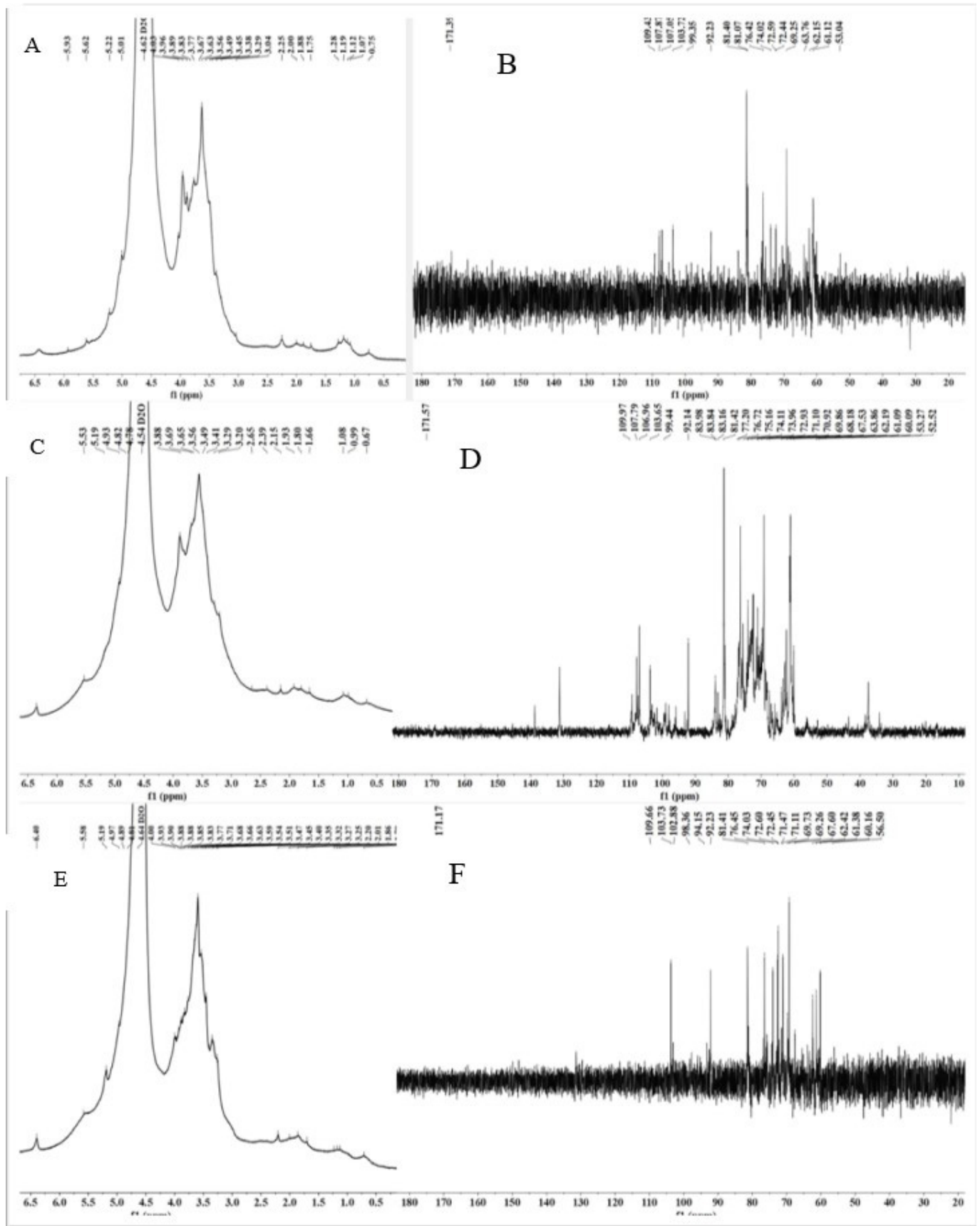


**Figure 5.** NMR spectrum of SLPs. (A) The  $^1\text{H}$  NMR spectrum of SLP-50, (B) the  $^{13}\text{C}$  NMR of SLP-50, (C) the  $^1\text{H}$  NMR spectrum of SLP-70, (D) the  $^{13}\text{C}$  NMR of SLP-70, (E) the  $^1\text{H}$  NMR spectrum of SLP-90, (F) the  $^{13}\text{C}$  NMR of SLP-90.

## TGA

Considering the frequent need for sterilization, thermal stability is an important parameter for bioactive molecules. The TGA curve is accompanied by the differential thermogravimetric (DTG) curve of the corresponding material. Small changes in mass were observed from 30 °C to 140 °C due to evaporation of water. The weight-loss pattern of the composite polymer of the SLPs with increasing temperature is shown in Figure 6. The results showed that SLP-50 and SLP-70 began to decompose at about 165 °C, while SLP-90 began to decompose at about 150 °C, and at 360 °C, the SLPs had lost about 40% of their weight due to polysaccharide ring dehydration and depolymerization (Hajji et al., 2019). The weight of SLP-70 and SLP-90 dropped sharply to 62% between 250 °C and 350 °C, while the weight of SLP-90 dropped sharply to 60% between 190 °C and 350 °C. Even if the temperature was raised to 600 °C, the SLPs retained about 45% of their residual mass, indicating good stability. The minimum DTG values of SLP-50, SLP-70, and SLP-90 were 309 °C, 304 °C, and 266 °C, respectively (degradation temperature). The thermograms showed that SLP-50, SLP-70, and SLP-90 exhibited maximum weight loss rates at 165 °C, 162 °C, and 150 °C, respectively,

and the order of thermal stability is SLP-50 > SLP-70 > SLP-90. The relatively high Mw of SLP-50 (36.40 kDa) may be the reason for its higher decomposition temperature; these results are similar to those of Jiang et al. (Jiang et al., 2020) in which the thermal stability of mung bean skin polysaccharide fraction MBP-2 (208 kDa) was higher than that of polysaccharide fraction MBP-1 (139 Da). In the DTG thermogram, the largest weight loss rate was observed for MBP-1 at 210 °C, while MBP-2 was stable up to 235 °C. These results are consistent with ours showing that SLP-50 had a more stable structure than SLP-70 and SLP-90, with good heat resistance at 247 °C.

## SEM analysis of SLPs

SEM images of SLPs were obtained to investigate the impact of gradient precipitation on the surface morphology of these polysaccharides. As shown in Figure 7, the appearance of the three polysaccharides fractions was loose, flaky, and wrinkled at 300× magnification, with holes in the structure and uneven distribution. This might be caused by turbulent shear, substantial cavitation activities, or instantaneous high pressure during the

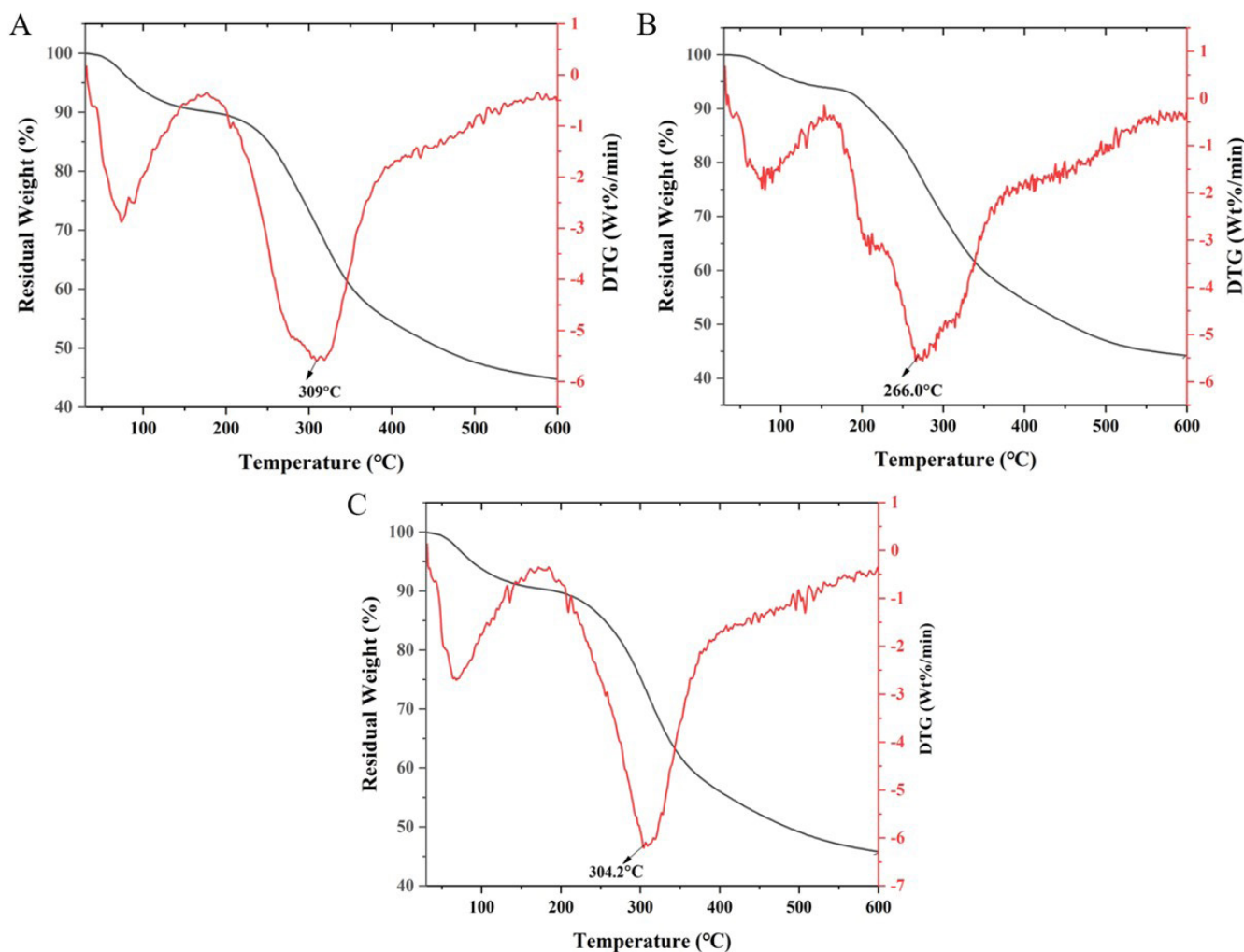


**Figure 6.** The curves of TGA and DTG of SLPs. (A) SLP-50; (B) SLP-70; (C) SLP-90.

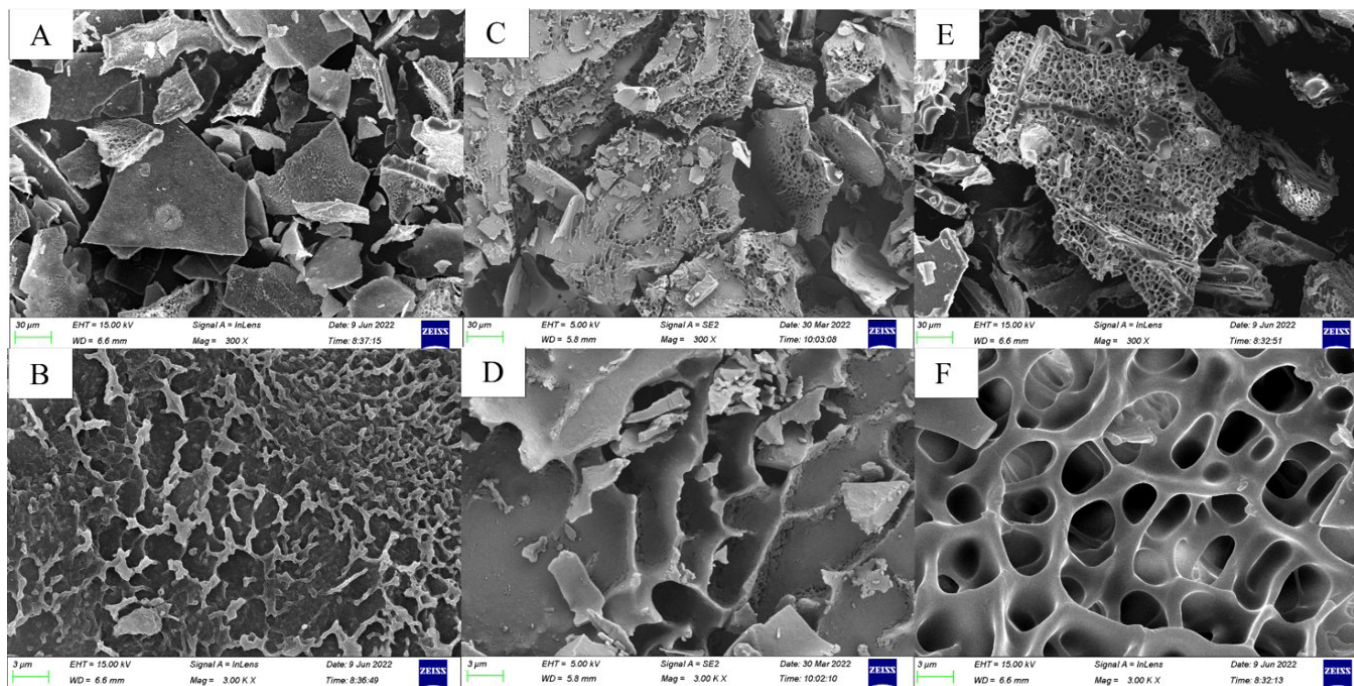


**Figure 7.** SEM images of SLP-50 (A,  $\times 300$ ; B,  $\times 3000$ ); SLP-70 (C,  $\times 300$ ; D,  $\times 3000$ ); SLP-90 (E,  $\times 300$ ; F,  $\times 3000$ ).

ultrasound extraction (Xu et al., 2018). At a magnification of 3000 $\times$ , the surface of SLP-50 appeared rough, with a 'curly' layered and dense structure, indicating that the polysaccharide molecules had a strong attraction to each other. SLP-70 contained many large honeycomb cavities, suggesting that there was repulsion between the polysaccharide molecules and that intermolecular attractions were weak. This may mean that the polysaccharide was not fully formed. A network-like structure can be found in SLP-90, which might have been formed by entanglement and cross-linking between polysaccharide molecules. SLP-90 also had a higher cavity density than the other two SLPs, suggesting that it had a larger branched structure, making it susceptible to cross linking (Wang et al., 2021a). These results indicate that ultrasound-assisted extraction with precipitation by different ethanol concentrations can affect intermolecular forces and alter the branching structure and crosslinking network of polysaccharides, endowing SLPs with different morphologies and appearances.

### 3.2. *In vitro* Antioxidant activity

#### *DPPH radical scavenging activity*

The DPPH radical is a stable free radical that has been frequently employed to assess the antioxidant capacity of polysaccharides (Yan et al., 2018). As shown in Figure 8A, the DPPH radical-scavenging capacity of SLPs increased in a concentration-dependent fashion. SLP-90 ( $IC_{50} = 47.55 \mu\text{g/mL}$ ) displayed greater DPPH radical scavenging ability than SLP-50 ( $IC_{50} = 108.52 \mu\text{g/mL}$ ) and SLP-70 ( $IC_{50} = 65.70 \mu\text{g/mL}$ ). At 0.12 mg/mL, the scavenging capacities of SLP-50, SLP-70, SLP-90, and Vc on the DPPH radical were 53.62%, 74.42%, 77.49%, and 81.07%, respectively, exhibiting a stronger antioxidant

effect than the GBLP<sub>2</sub> polysaccharides from *Ginkgo biloba* leaves (Wang et al., 2022); the scavenging activity of GBLP<sub>2</sub> on DPPH was 52.67% at 0.5 mg/mL. The antioxidant effect of polysaccharides has been related to their molecular weight, monosaccharide composition, and chemical composition (Shen et al., 2014). Generally, the DPPH radical scavenging capability of polysaccharides depends on their ability to donate electrons or hydrogen. The SLPs displayed different molecular weights and monosaccharide compositions, which might result in differences in the glucosidic bonds and the configurations and sequence of monosaccharides, resulting in a significant impact on their hydrogen-donating capacities (Chen et al., 2011). For example, SLP-90 might have greater hydrogen-donating capacity compared to the other two SLPs, thereby scavenging DPPH radicals more effectively. Uronic acid groups in polysaccharides could activate hydrogen atoms on anomeric carbons (Chen et al., 2019a), and the higher antioxidant activity of SLP-90 could be the result of its greater uronic acid content. In addition to this, the abundant network structure and larger zeta potential of SLP-90 may contribute to better antioxidant activity. Chen et al. extracted polysaccharides from *Bletilla striata* by different methods and found that they contained a network structure more favorable for active site exposure (Chen et al., 2021b). Gu et al. (2020) studied polysaccharides extracted from *Sagittaria sagittifolia* with different zeta potentials (|10.74–15.88|) and determined that polysaccharides with higher zeta potential had higher antioxidant activity (Gu et al., 2020a). Our results are in good agreement with these reports. The maximum scavenging effect of SLP-90 (77.49%) reached 81.07% of Vc (95.58%), indicating that it was feasible to prepare SLPs with strong DPPH radical scavenging ability by our ultrasonic extraction method.

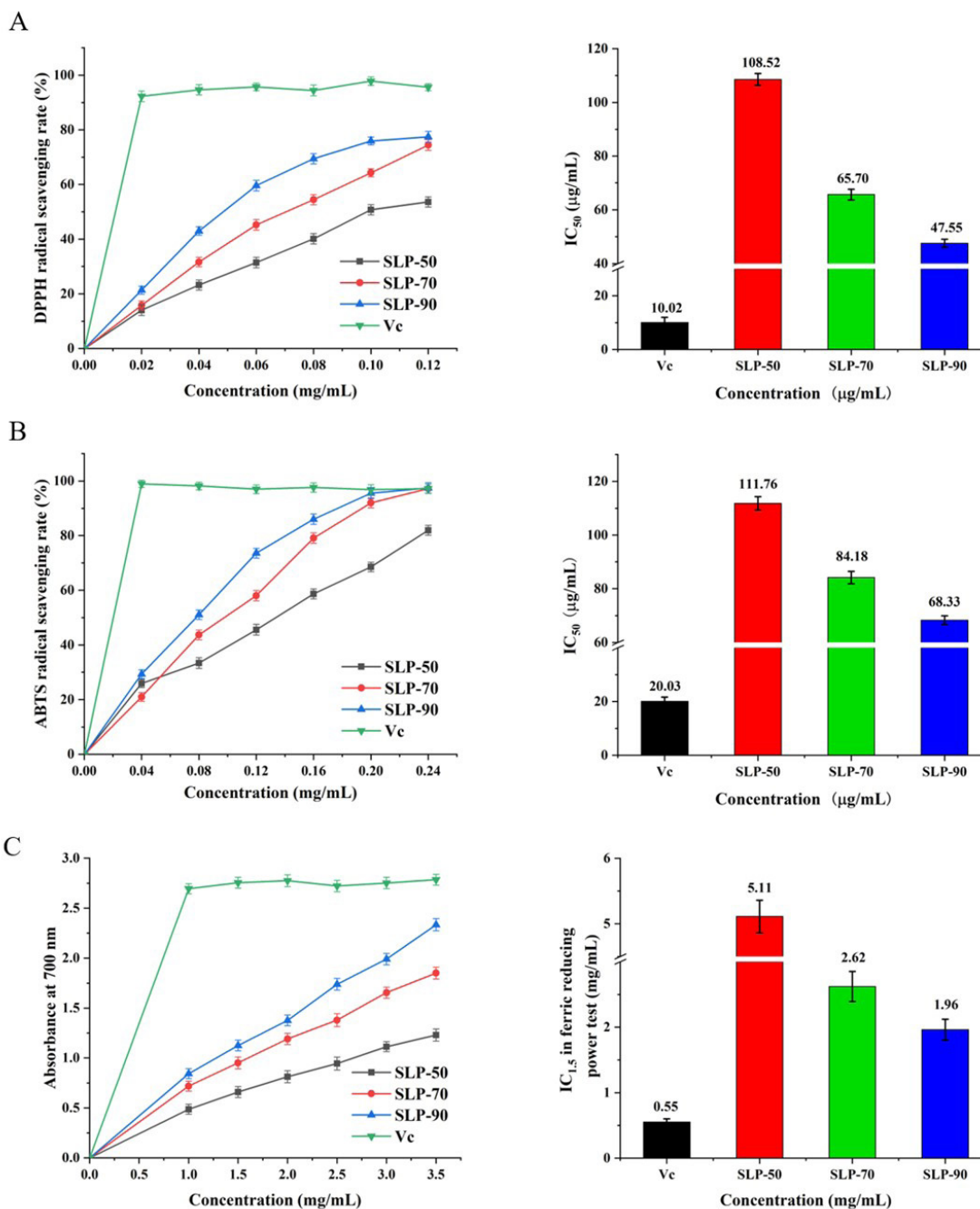


**Figure 8.** Antioxidant activity of SLPs *in vitro*. (A): DPPH radical scavenging assay and IC<sub>50</sub> in DPPH radical scavenging assay; (B): ABTS radical scavenging assay and IC<sub>50</sub> in ABTS radical scavenging assay; (C): Reducing power assay and IC<sub>1.5</sub> in ferric reducing power. The values are reported as the mean ± SD of three replicate studies.

#### ABTS radical scavenging activity

The ABTS free radical can react with antioxidants by absorbing electrons or hydrogen atoms (Khaskheli et al., 2015), which indirectly reflects the antioxidant potential of polysaccharides. Our SLPs scavenged ABTS radical in a dose-dependent manner (Figure 8B). SLP-90 (IC<sub>50</sub> = 68.33 μg/mL) had stronger ABTS radical scavenging activity than SLP-50 (IC<sub>50</sub> = 111.76 μg/mL) and SLP-70 (IC<sub>50</sub> = 84.18 μg/mL). Zhang et al. prepared three new

polysaccharides (MLP1, MLP2, and MLP3) from mulberry leaves by ultrasound extraction (Zhang et al., 2016). The scavenging capability of 1 mg/mL MLP1, MLP2, and MLP3 on ABTS radicals was 42.36%, 25.00%, and 15.59%, respectively, which was substantially weaker than that of SLPs. The ABTS radical scavenging ability of SLP-90 sharply increased with increasing concentrations, which might be a result of its higher rhamnose content (7.41%), a key indicator of antioxidant activity (Gu et al., 2020b). In addition, the high total phenolics content of SLP-

90 (8.23%) could also contribute to its strong antioxidant activity. SLP-90 can generate a stable semiquinone structure and terminate the free radical chain-reaction via reaction of the phenolic hydroxyl group with free radicals. The presence of a higher protein content in SLP-90 (3.35%) might also have a synergistic effect on antioxidant activity because proteins contain strong reducing groups, such as carboxyls, which can act as hydrogen or electron donors (Bai et al., 2022). This finding suggests that the formation of polysaccharide conjugates with phenolic compounds and proteins could have a significant synergistic effect on the overall antioxidant activity (Wu et al., 2022). Notably, at 0.24 mg/mL, the scavenging ability of SLP-90 (97.45%) surpassed the scavenging level of Vc (97.17%), demonstrating that SLP-90 had a substantial ABTS radical scavenging capability and could be applicable as a potential novel antioxidant.

#### Reducing power

Fe (III) reduction could serve as an indicator to measure the electron-donating ability, which could predict the potential antioxidant activity of polysaccharides (Khaskheli et al., 2015). As illustrated in Figure 8C, the reducing power of the three SLPs and Vc exhibited a positive correlation with increasing concentration, and the order of reducing power was: SLP-90 > SLP-70 > SLP-50, indicating that SLP-90 was the best electron donor and could effectively inhibit oxidative chain reactions. At 3.5 mg/mL, the reducing power of SLP-50, SLP-70, SLP-90 reached 1.23, 1.85, and 2.33, respectively. The  $IC_{1.5}$  of SLP-50, SLP-70 and SLP-90 was 5.11, 2.62, and 1.96 mg/mL, respectively, which showed much lower reducing power than Vc ( $IC_{1.5} = 0.55$  mg/mL). However, SLP-70 and SLP-90 displayed higher reducing power than that reported by Chen et al. (2021a). The above researchers obtained two polysaccharides (DF-GSLP and TF-GSLP) from ginger leaves, but the absorbance of DF-GSLP and TF-GSLP was still less than 1.5 when the concentration reached 3 mg/mL. SLP-90 displayed the strongest reducing power, possibly because of its lower Mw. Some reports claimed that, among the properties affecting antioxidant activity of polysaccharides, Mw was the major element because the same mass of polysaccharides with smaller Mw's carried more reductant hydroxyl terminals to accept and eliminate free radicals than polysaccharides with high Mw's (Wu et al., 2022). In addition, the antioxidant properties of polysaccharides are not composed of a single factor; other elements, such as glycosidic linkages may also have a key impact on the antioxidant capacity of polysaccharides. Changes in glycosidic bonds alter the steric conformation of the polysaccharide, thereby affecting the exposure of hydroxyl groups (Wu et al., 2022). This change could have a substantial effect on the hydrogen-donating capability of polysaccharides, thereby affecting their antioxidant activity. The actual mechanism by which the glycosidic bond affected the antioxidant activity needs additional study. The results indicated that improving the ferric ion reducing power of polysaccharides could be accomplished by increasing the volume fraction of ethanol used for polysaccharide precipitation, probably because increasing the ethanol concentration increased the number of hydrogen donors (Wang et al., 2016).

### 3.3 *In vitro* hypoglycemic activity

Inhibiting carbohydrate-hydrolyzing enzymes such as  $\alpha$ -amylase and  $\alpha$ -glucosidase is a common strategy for lowering postprandial hyperglycemia (Zhang et al., 2020a). Therefore,  $\alpha$ -amylase and  $\alpha$ -glucosidase inhibition tests could be considered as simple and efficient methods for determining the *in vitro* hypoglycemic activity of bioactive compounds. The three SLPs and acarbose exhibited concentration-dependent inhibitory effects on the two enzymes (Figure 9). The  $IC_{50}$  values of acarbose, SLP-50, SLP-70, and SLP-90 were 2.60, 12.22, 6.52 and 6.93 mg/mL on  $\alpha$ -amylase, and 0.80, 0.11, 0.05 and 0.67 mg/mL on  $\alpha$ -glucosidase, respectively. The  $IC_{50}$  values of the three fractions on  $\alpha$ -glucosidase were much lower than those of polysaccharides FD-MSP, VD-MSP and MSP obtained from *Medicago sativa L.* (9.73, 11.40, and 13.98 mg/mL) (Shang et al., 2021). Results showed that SLP-70 had considerably higher inhibitory effects for  $\alpha$ -amylase and  $\alpha$ -glucosidase than SLP-50 and SLP-90. SLPs exhibited a stronger inhibitory effect on  $\alpha$ -glucosidase than acarbose but a weaker inhibitory effect on  $\alpha$ -amylase than acarbose. This disparity might be attributed to the differences in molecular conformation, monosaccharide composition, Mw, glycosyl linkage type, and uronic acid content of derived fractions (Cui et al., 2015). It has been suggested that polysaccharide structures with a higher content of xylose or arabinose residues greatly inhibited  $\alpha$ -amylase and  $\alpha$ -glucosidase (Lv et al., 2021). Moreover, some researchers reported that through hydrogen bonding, the structural groups of carboxylic acids and hydroxyls on the branching chains of polysaccharides might interact significantly with the enzymes' catalytic residues. These polysaccharide-enzyme complexes may effectively inhibit the activities of  $\alpha$ -amylase and  $\alpha$ -glucosidase, and low-Mw polysaccharides have better inhibitory activities due to more active site exposure and less transmembrane resistance (Cao et al., 2018).

In this study, SLP-70 showed a larger content of arabinose (18.87%) and xylose (11.62%) than SLP-90 (9.96% and 8.97%). Compared to SLP-50 (36.40 kDa and 4.21%), SLP-70 displayed lower Mw (12.97 kDa) and higher uronic acid content (4.96%). These factors could have contributed to the stronger  $\alpha$ -amylase and  $\alpha$ -glucosidase inhibition of SLP-70. In addition, the amounts of SLPs required to inhibit  $\alpha$ -amylase were much higher than for  $\alpha$ -glucosidase, which suggests that SLPs had stronger inhibitory effects on  $\alpha$ -glycosidase than on  $\alpha$ -amylase. Similarly, Zhao et al. found that *Dioscorea* polysaccharides had strong hypoglycemic activity *in vitro*; however, the amount required to inhibit  $\alpha$ -amylase ( $IC_{50} = 3.66 - 47.57$  mg/mL) was much higher than that required for  $\alpha$ -glucosidase ( $IC_{50} = 27.41 - 274.36$   $\mu$ g/mL) (Zhao et al., 2017). In contrast, Li et al. found that *Sargassum* polysaccharides exhibited weaker inhibitory effects on  $\alpha$ -glucosidase than  $\alpha$ -amylase (Li et al., 2017a). This variation was probably owing to the different mechanisms of action between  $\alpha$ -amylase and  $\alpha$ -glycosidase (Yan et al., 2018). Because of structural differences in the binding site and active site between  $\alpha$ -amylase and  $\alpha$ -glucosidase, SLPs may be able to interact more fully with  $\alpha$ -glucosidase leading to significant changes in some conformations of the enzyme molecule, possibly disrupting secondary bonds, and thereby reducing the activity of the enzyme (Cho et al., 2011). Therefore, based on the above results, we concluded that SLP-70 had outstanding hypoglycemic

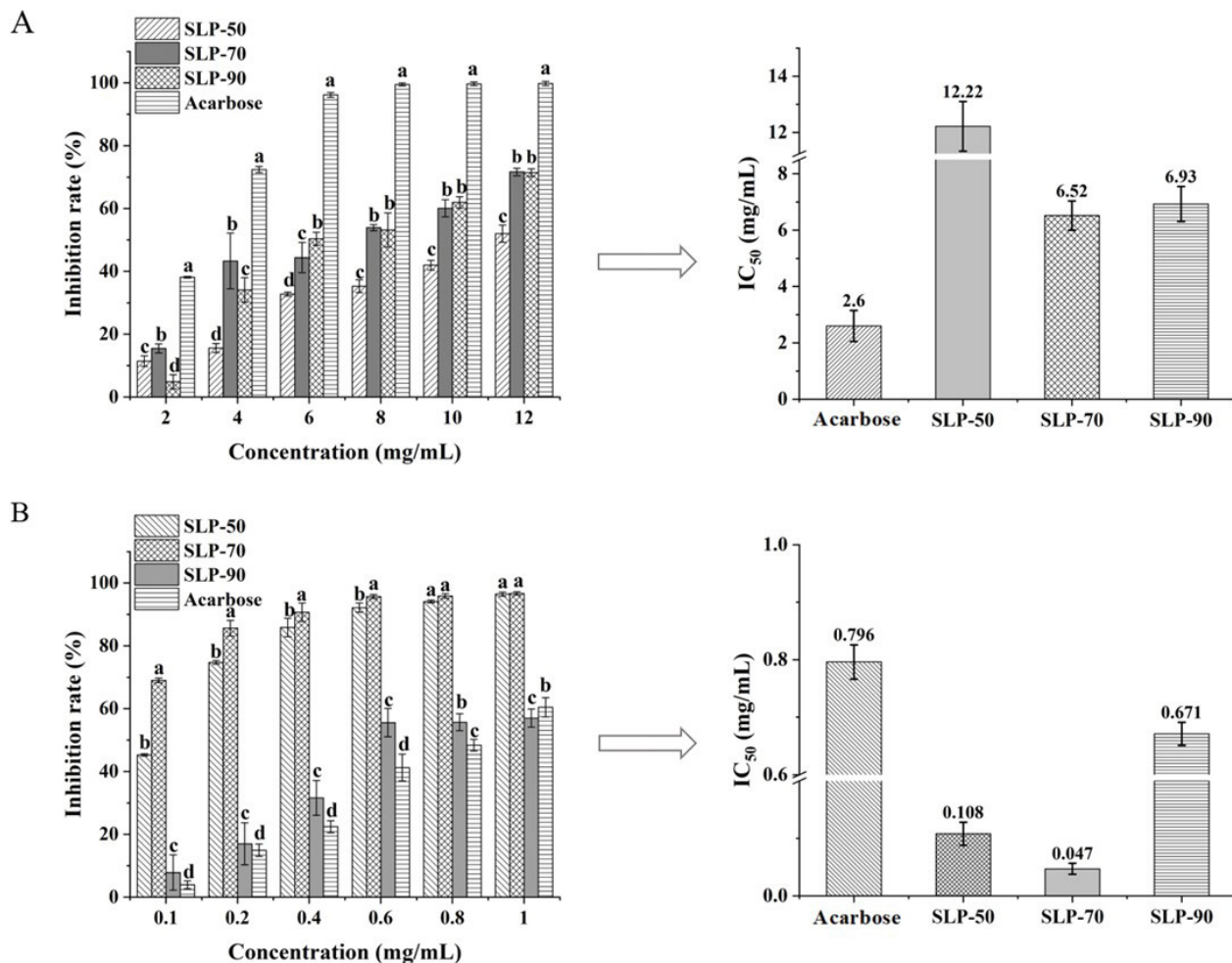


**Figure 9.** Hypoglycemic activities of SLP-50, SLP-70, and SLP-90 *in vitro*. (A):  $\alpha$ -amylase inhibition assay and  $IC_{50}$  in  $\alpha$ -amylase inhibition test; (B):  $\alpha$ -glucosidase inhibition assay and  $IC_{50}$  in  $\alpha$ -glucosidase inhibition assay. The values are reported as the mean  $\pm$  SD of triple trials, and different letters for the same concentration denote significant differences at  $p < 0.05$ .

activity compared to SLP-50 and SLP-90; it could be exploited as a prospective hypoglycemic drug or functional food supplement.

### 3.4 Antibacterial activity

Since bacteria have become resistant to many antibiotics, controlling bacterial infection has become a serious concern. Accordingly, research into novel natural materials containing antibacterial properties has lately expanded (Hajji et al., 2019). In this study, the bacteriostatic activity of SLPs was evaluated against three Gram-negative bacteria (*P. aeruginosa*, *S. typhimurium*, and *E. coli*) and one Gram-positive bacterium (*S. aureus*). The SLPs all had pronounced inhibitory effects on each bacterium (Figure 10a). As shown in Table 2, both SLP-50 and SLP-70 displayed high inhibitory activity against four bacterial strains (inhibition zones  $>20$  mm). In contrast, SLP-90 showed various degrees of inhibitory effects on different bacteria. It exhibited high inhibitory activities against *P. aeruginosa* ( $21.07 \pm 2.76$  mm), moderate inhibitory activity against *S. typhimurium* ( $19.50 \pm 0.96$  mm) and *E. coli* ( $18.47 \pm 1.62$  mm),

and weak to moderate inhibition of *S. aureus* ( $13.73 \pm 1.45$  mm). At 1 mg/mL, the antimicrobial effects of SLPs decreased in the order: SLP-50  $>$  SLP-70  $>$  SLP-90. In comparison, polysaccharides from *Cyclocarya paliurus* leaves showed significantly weaker antimicrobial activity than SLPs, and its inhibition zones against *S. aureus* and *E. coli* were only  $6.57 \pm 0.11$  and  $6.54 \pm 0.23$  mm at 1 mg/mL, respectively (Hojjati & Beirami-Serizkani, 2020). Polysaccharides from olive leaves also exhibited significant antibacterial activity; however, their antibacterial effects were weaker than those of the SLPs; the *E. coli* inhibition zone was only  $10.50 \pm 0.71$  mm at 50 mg/mL (Khemakhem et al., 2018). SLP-50 had a lower MIC value than the other two SLPs against all four strains, while the MIC of SLP-50 against *E. coli* was higher than that of polysaccharide EAP60-1 from the leaves of *Epimedium acuminatum* (0.25 mg/mL) (Cheng et al., 2013). In general, the antibacterial activity of polysaccharides is affected by monosaccharide compositions, total sugar content, specific structure, and conformational characteristics (Zhou et al., 2022). The strong antibacterial effect of the three SLPs might be associated with their numerous sulfate groups. In addition,

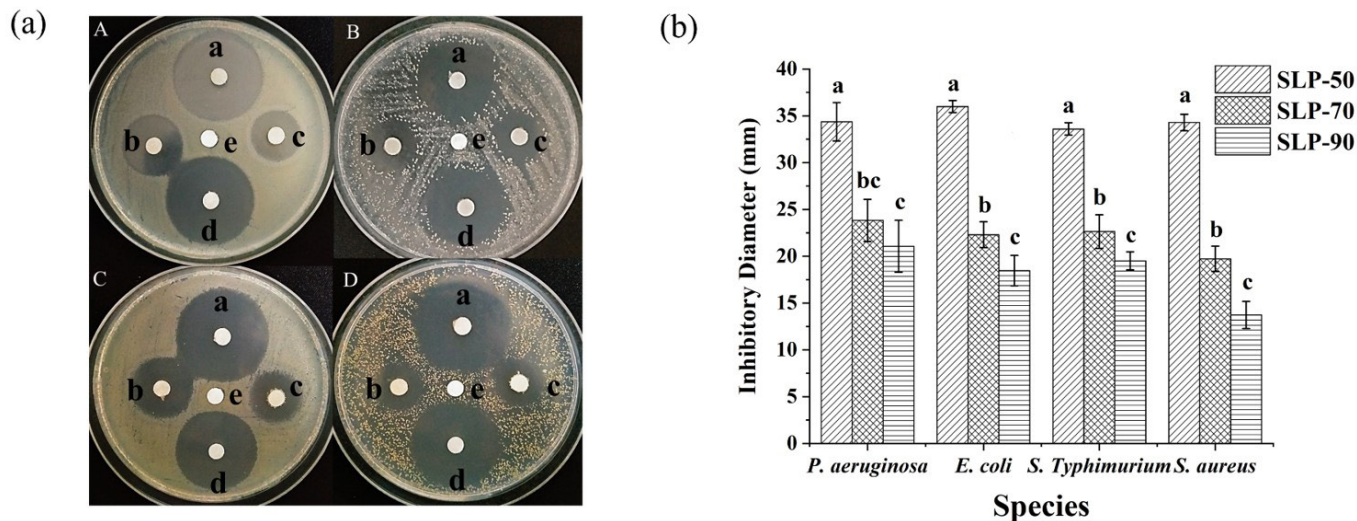


**Figure 10.** Inhibition zone diameter of SLPs at 1mg/mL against A (*P. aeruginosa*), B (*S. typhimurium*), C (*E. coli*), and D (*S. aureus*). a, b, c, d, e were the inhibition zones (mm) of SLP-50, SLP-70, SLP-90, positive control (levofloxacin) (50 µg/mL), and negative control (water), respectively (a); The inhibitory effect of SLPs at 1mg/mL on four bacteria. For diverse SLPs to the same microorganism, different letters denote significant differences at  $p < 0.05$  (b).

**Table 2.** The antibacterial activity of SLP-50, SLP-70, and SLP-90.

| Bacteria strains      | Inhibition zones (mm, 1 mg/mL polysaccharide) |                |               |               | MICs (mg/mL) |        |        |              |
|-----------------------|---|----------------|---------------|---------------|--------------|--------|--------|--------------|
|                       | SLP-50  | SLP-70         | SLP-90        | Levofloxacin  | SLP-50       | SLP-70 | SLP-90 | Levofloxacin |
| <i>P. aeruginosa</i>  | 34.37 ± 2.05a                                 | 23.83 ± 2.24bc | 21.07 ± 2.76c | 32.52 ± 1.33a | 0.63         | 1.25   | 2.50   | <0.04        |
| <i>S. Typhimurium</i> | 33.61 ± 0.67a                                 | 22.63 ± 1.80b  | 19.50 ± 0.96c | 32.87 ± 0.89a | 0.63         | 1.25   | 2.50   | <0.04        |
| <i>E. coli</i>        | 36.00 ± 0.65a                                 | 22.30 ± 1.37c  | 18.47 ± 1.62d | 33.01 ± 0.79b | 0.31         | 1.25   | 2.50   | <0.04        |
| <i>S. aureus</i>      | 34.30 ± 0.88a                                 | 19.73 ± 1.36b  | 13.73 ± 1.45c | 32.32 ± 0.78a | 0.63         | 2.50   | 3.13   | <0.04        |

Values of inhibition zones are indicated as mean ± SD (n=3). Means are significantly different with the different letters in the same row ( $p < 0.05$ ).

the polyphenol moieties in SLPs may have synergistic effects. The stronger antibacterial effect of SLP-50 might be attributed to its higher content of total sugar (50.54%) and sulfate groups (38.94%) compared to SLP-70 and SLP-90. It is worth noting that the thermal stability of SLP-50 is greater than that of SLP-70 and SLP-90, which may also contribute to its stronger antibacterial activity. The higher thermal stability of SLP-50 could greatly reduce the escape of active ingredients (Zhang et al., 2020b).

Figure 10b shows the antimicrobial activities of the SLPs at 1 mg/mL against different bacteria at, and the results indicated that Gram-negative bacteria were more sensitive to SLPs than Gram-positive bacteria, probably because Gram-positive bacteria have thicker peptidoglycan walls and relatively higher drug resistance. SLPs could more easily diffuse through the lipopolysaccharides of Gram-negative bacteria, thus exerting a greater antibacterial effect (Zhou et al., 2022). The high sulfate content of SLPs might also be a factor in producing the enhanced killing effect on Gram-negatives (Liu et al., 2017). Our results were in agreement with previous studies of *Hypericum perforatum* polysaccharides, in which the Gram-negative *E. coli* and *S. typhi* were more sensitive than *S. aureus* and *B. cereus* (Gram-positives) (Heydari et al., 2017). However, Hashemifesharaki et al. found that the inhibitory

activity of polysaccharides from *Althaea officinalis* (MRP-P1) against Gram-positive bacteria (*S. aureus*) was higher than that of Gram-negative bacteria (*E. coli*) (Hashemifesharaki et al., 2020). The reason for this difference may be that different plant sources contain polysaccharides with different properties (Li et al., 2018).

According to the antibacterial zone-of-inhibition and MICs results, SLP-50 (10 mg/mL) had the highest activity and was selected for further study of its antibacterial activity by SEM, with *S. aureus* (Gram+) and *E. coli* (Gram-) as targets. The morphological characteristics of treated and untreated *S. aureus* and *E. coli* are shown in Figure 11. These images show the apparent destructive effects of SLP-50 on the tested bacteria. *S. aureus* in the normal state was regular, spherical, and intact, with a smooth surface. After treatment with SLP-50, the surface of *S. aureus* presented a collapsed appearance, wrinkled and uneven in form, and surrounded by drug exudates. Untreated *E. coli* are regular short rods or cylinders with an intact and smooth surface. Following a 6-h incubation with SLP-50, the surface of *E. coli* exhibited folds, irregular shapes and cylindrical crevices, with hollow structures at both ends surrounded by drug exudates. The cell walls and membranes were degraded allowing leakage of cytoplasmic contents, which suggested that the antimicrobial mechanism might be due to

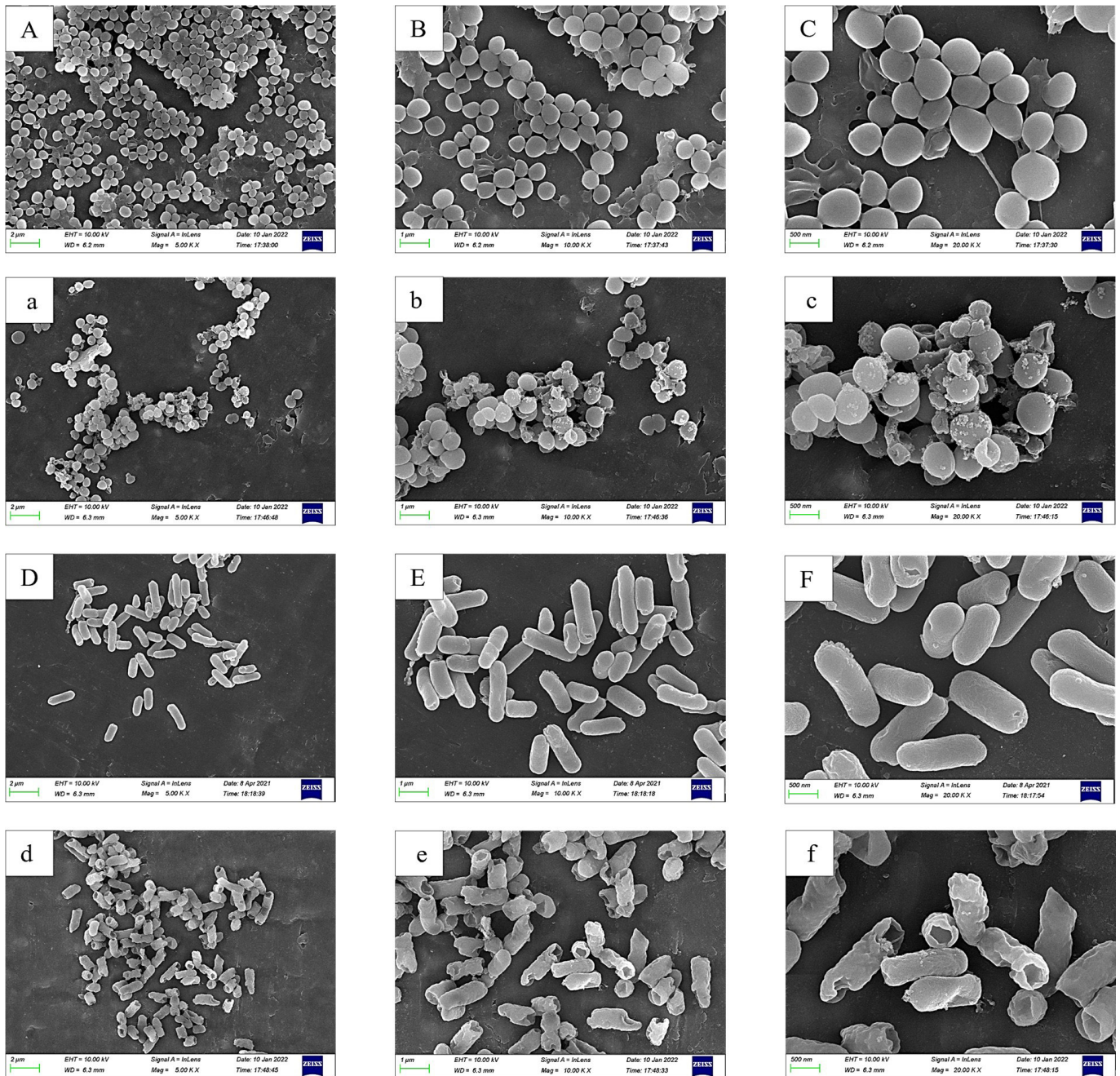


**Figure 11.** SEM images of *S. aureus* and *E. coli*. *S. aureus* and *E. coli* without SLP-50 treatment were represented by A (2  $\mu$ m), B (1  $\mu$ m), C (500 nm), and D (2  $\mu$ m), E (1  $\mu$ m), F (500 nm), respectively; *S. aureus* and *E. coli* with SLP-50 treatment were represented by a (2  $\mu$ m), b (1  $\mu$ m), c (500 nm), and d (2  $\mu$ m), e (1  $\mu$ m), f (500 nm), respectively (c).

disruption of the cell wall and membrane, leading to loss of contents and death (Zhang et al., 2020b). Chen et al. studied the complex antimicrobial mechanism of polysaccharides from *Tetrastigma hemsleyanum* Diels et Gilg, and determined that it was not a simple result of membrane disruption because these polysaccharides blocked *E. coli* proliferation by hindering the phosphorylation of glucose and interfering with glycolysis and gluconeogenesis. The antibacterial effects of SLP-50 could be mainly associated with its abundant negatively charged sulfate groups (38.94%), which enable the polysaccharides to bind

cationic nutrients, thereby decreasing the bacteria's nutritional intake (Zhou et al., 2022). The sulfates in polysaccharides might also circumvent resistance mechanisms, such as the pump-mediated efflux systems and resistance genes, leading to penetration of cell walls and membranes, downregulation of gene expression, inhibition of the bacterial DNA damage response and death (Aruwa et al., 2022). In addition, the polyphenols in SLP-50 that synergistically act with antibacterial compounds can impart hydrophobic properties and inhibit the cross-linking step of cell wall synthesis by forming labile

complexes that bind to cell wall proteins and enzymes. Inhibition of cell wall synthesis causes structural changes in microbial membranes, leading to increased cell membrane permeability, allowing SLP-50 to passively diffuse into the cytosol, and causing changes to bacterial enzyme systems and escape of intracellular components. This accelerating leakage of cellular components such as proteins, glutamate, and nucleic acids, promotes the influx of more antimicrobial compounds including phenolics, which increase hyperpolarization and disruption of lipid-protein interactions (Zhou et al., 2022). It is likely that even more complex molecular mechanisms and structure-function relationships remain to be elucidated.

#### 4 Conclusion

It has been proven that the three polysaccharide fractions (SLP-50, SLP-70 and SLP-90) isolated from sugarcane leaves by ultrasound-assisted fractional ethanol precipitation are natural antioxidants, hypoglycemic agents, and antibacterial compounds. Each fraction has its own unique characteristics related to the physicochemical properties: SLP-90 is the strongest antioxidant, SLP-70 has the highest hypoglycemic activity, and SLP-50 has the greatest antibacterial properties. The analytical results showed that the SLPs were acidic heteropolysaccharides composed of Mannose, rhamnose, glucuronic acid, galacturonic acid, glucose, galactose, arabinose and xylose, and that the molar ratios were significantly different. Compared to the other two polysaccharides, SLP-90 has the lowest molecular weight and the most extensive cavity structure, which provides a larger number of active sites for binding free radicals. The higher uronic acid content in SLP-90 also activates hydrogen atoms on its anomeric carbon, thereby enabling it to rapidly react with free radicals to terminate the free radical chain reaction. SLP-70 has the highest content of arabinose and xylose, which allows it to inhibit  $\alpha$ -amylase and  $\alpha$ -glucosidase. SLP-50 has the highest Mw, which provides it with the greatest thermostability. In addition, SLP-50 has the highest content of total sugar and charged sulfate groups, which allows it to exert the strongest antibacterial ability. Our findings indicated that ultrasound-assisted fractional ethanol precipitation is an effective, scalable extraction technique for producing bioactive polysaccharides from sugarcane leaves. The polysaccharide fractions have broad potential applicability in the food and pharmaceutical industries. Further detailed structural studies of the sugarcane leaves polysaccharides by periodate oxidation, Smith degradation, methylation and NMR are in progress.

#### Declaration of competing interest

The authors declare that there are no competing financial interests in this study.

#### CRedit authorship contribution statement

**Mengmiao Mo:** Investigation, Formal analysis, Data curation, Writing – original draft. **Weiming Chen:** Editing, Visualization. **Fengyu Jiang:** Conceptualization, Data curation. **Zhendong Ding:** Writing – review. **Yongguang Bi:** Validation, Formal analysis. **Fansheng Kong:** Writing – review & editing, Project administration.

#### Acknowledgements

This work was supported by the Project of Guangdong Provincial Department of Education-special projects in key areas (grant numbers: 2021ZDZX4013) and Scientific Research Project of Guangdong Provincial Bureau of Traditional Chinese Medicine (20231216).

#### References

- Ali, S. E., Yuan, Q., Wang, S., & Farag, M. A. (2021). More than sweet: A phytochemical and pharmacological review of sugarcane (*Saccharum officinarum* L.). *Food Bioscience*, 44, 101431. <http://dx.doi.org/10.1016/j.fbio.2021.101431>.
- Aruwa, C. E., Amoo, S. O., Koorbanally, N., & Kudanga, T. (2022). Laccase-mediated modification of isorhamnetin improves antioxidant and antibacterial activities. *Process Biochemistry*, 112, 53-61. <http://dx.doi.org/10.1016/j.procbio.2021.11.019>.
- Bai, C., Chen, R., Tan, L., Bai, H., Tian, L., Lu, J., Gao, M., Sun, H., & Chi, Y. (2022). Effects of multi-frequency ultrasonic on the physicochemical properties and bioactivities of polysaccharides from different parts of ginseng. *International Journal of Biological Macromolecules*, 206, 896-910. <http://dx.doi.org/10.1016/j.ijbiomac.2022.03.098>. PMID:35318082.
- Ban, J., Chen, J., Hu, X., Xu, X., Fu, J., Meng, F., & Wang, F. (2013). Extraction and separation of sugarcane intrinsic polysaccharide and analysis of monosaccharide composition. *Shipin Kexue*, 34(20), 182-185.
- Cao, C., Huang, Q., Zhang, B., Li, C., & Fu, X. (2018). Physicochemical characterization and in vitro hypoglycemic activities of polysaccharides from *Sargassum pallidum* by microwave-assisted aqueous two-phase extraction. *International Journal of Biological Macromolecules*, 109, 357-368. <http://dx.doi.org/10.1016/j.ijbiomac.2017.12.096>. PMID:29273524.
- Chen, G., Fang, C., Ran, C., Tan, Y., Yu, Q., & Kan, J. (2019a). Comparison of different extraction methods for polysaccharides from bamboo shoots (*Chimonobambusa quadrangularis*) processing by-products. *International Journal of Biological Macromolecules*, 130, 903-914. <http://dx.doi.org/10.1016/j.ijbiomac.2019.03.038>. PMID:30849468.
- Chen, G., Li, C., Wang, S., Mei, X., Zhang, H., & Kan, J. (2019b). Characterization of physicochemical properties and antioxidant activity of polysaccharides from shoot residues of bamboo (*Chimonobambusa quadrangularis*): effect of drying procedures. *Food Chemistry*, 292, 281-293. <http://dx.doi.org/10.1016/j.foodchem.2019.04.060>. PMID:31054677.
- Chen, H., Zeng, J., Wang, B., Cheng, Z., Xu, J., Gao, W., & Chen, K. (2021). Structural characterization and antioxidant activities of *Bletilla striata* polysaccharide extracted by different methods. *Carbohydrate Polymers*, 266, 118149. <http://dx.doi.org/10.1016/j.carbpol.2021.118149>. PMID:34044956.
- Chen, X., Wang, Z., & Kan, J. (2021a). Polysaccharides from ginger stems and leaves: effects of dual and triple frequency ultrasound assisted extraction on structural characteristics and biological activities. *Food Bioscience*, 42, 101166. <https://doi.org/10.1016/j.fbio.2021.101166>.
- Chen, R., Liu, Z., Zhao, J., Chen, R., Meng, F., Zhang, M., & Ge, W. (2011b). Antioxidant and immunobiological activity of water-soluble polysaccharide fractions purified from *Acanthopanax senticosu*. *Food Chemistry*, 127(2), 434-440. <http://dx.doi.org/10.1016/j.foodchem.2010.12.143>. PMID:23140683.
- Chen, X., Jia, X., Yang, S., Zhang, G., Li, A., Du, P., Liu, L., & Li, C. (2022). Optimization of ultrasonic-assisted extraction of flavonoids,

- polysaccharides, and eleutherosides from *Acanthopanax senticosus* using response surface methodology in development of health wine. *LWT*, 165, 113725. <http://dx.doi.org/10.1016/j.lwt.2022.113725>.
- Cheng, H., Feng, S., Shen, S., Zhang, L., Yang, R., Zhou, Y., & Ding, C. (2013). Extraction, antioxidant and antimicrobial activities of *Epimedium acuminatum* Franch. polysaccharide. *Carbohydrate Polymers*, 96(1), 101-108. <http://dx.doi.org/10.1016/j.carbpol.2013.03.072>. PMID:23688459.
- Cho, M., Han, J. H., & You, S. (2011). Inhibitory effects of fucan sulfates on enzymatic hydrolysis of starch. *Lebensmittel-Wissenschaft + Technologie*, 44(4), 1164-1171. <http://dx.doi.org/10.1016/j.lwt.2010.09.019>.
- Chou, C. H., Sung, T. J., Hu, Y. N., Lu, H. Y., Yang, L. C., Cheng, K. C., Lai, P. S., & Hsieh, C. W. (2019). Chemical analysis, moisture-preserving, and antioxidant activities of polysaccharides from *Pholiota nameko* by fractional precipitation. *International Journal of Biological Macromolecules*, 131, 1021-1031. <http://dx.doi.org/10.1016/j.ijbiomac.2019.03.154>. PMID:30910671.
- Cui, J., Gu, X., Wang, F., Ouyang, J., & Wang, J. (2015). Purification and structural characterization of an  $\alpha$ -glucosidase inhibitory polysaccharide from apricot (*Armeniaca sibirica* L. Lam.) pulp. *Carbohydrate Polymers*, 121, 309-314. <http://dx.doi.org/10.1016/j.carbpol.2014.12.065>. PMID:25659703.
- Fakhfakh, N., Abdelhedi, O., Jdir, H., Nasri, M., & Zouari, N. (2017). Isolation of polysaccharides from *Malva aegyptiaca* and evaluation of their antioxidant and antibacterial properties. *International Journal of Biological Macromolecules*, 105(Pt 2), 1519-1525. <http://dx.doi.org/10.1016/j.ijbiomac.2017.07.105>. PMID:28732725.
- Fu, Y., Li, F., Ding, Y., Li, H. Y., Xiang, X. R., Ye, Q., Zhang, J., Zhao, L., Qin, W., Gan, R. Y., & Wu, D. T. (2020). Polysaccharides from loquat (*Eriobotrya japonica*) leaves: Impacts of extraction methods on their physicochemical characteristics and biological activities. *International Journal of Biological Macromolecules*, 146, 508-517. <http://dx.doi.org/10.1016/j.ijbiomac.2019.12.273>. PMID:31923490.
- Gu, J., Zhang, H., Yao, H., Zhou, J., Duan, Y., & Ma, H. (2020a). Comparison of characterization, antioxidant and immunological activities of three polysaccharides from *Sagittaria sagittifolia* L. *Carbohydrate Polymers*, 235, 115939. <http://dx.doi.org/10.1016/j.carbpol.2020.115939>. PMID:32122481.
- Gu, J., Zhang, H., Zhang, J., Wen, C., Ma, H., Duan, Y., & He, Y. (2020b). Preparation, characterization and bioactivity of polysaccharide fractions from *Sagittaria sagittifolia* L. *Carbohydrate Polymers*, 229, 115355. <http://dx.doi.org/10.1016/j.carbpol.2019.115355>. PMID:31826432.
- Gui, Y., Xian, W., Liang, Q., Su, S., & Yang, R. (2012). Extraction and antioxidant activity of polysaccharides from Sugarcane leaves in vitro. *Journal of Southwest Agricultural University*, 25(04), 1218-1221.
- Hajji, M., Hamdi, M., Sellimi, S., Ksouda, G., Laouer, H., Li, S., & Nasri, M. (2019). Structural characterization, antioxidant and antibacterial activities of a novel polysaccharide from *Periploca laevigata* root barks. *Carbohydrate Polymers*, 206, 380-388. <http://dx.doi.org/10.1016/j.carbpol.2018.11.020>. PMID:30553336.
- Hardinasinta, G., Mursalim, M., Muhidong, J., & Salengke, S. (2022). Degradation kinetics of anthocyanin, flavonoid, and total phenol in bignay (*Antidesma bunius*) fruit juice during ohmic heating. *Food Science and Technology (Campinas)*, 42, e64020. <http://dx.doi.org/10.1590/fst.64020>.
- Hashemifesharaki, R., Xanthakis, E., Altintas, Z., Guo, Y., & Gharibzahedi, S. M. T. (2020). Microwave-assisted extraction of polysaccharides from the marshmallow roots: optimization, purification, structure, and bioactivity. *Carbohydrate Polymers*, 240, 116301. <http://dx.doi.org/10.1016/j.carbpol.2020.116301>. PMID:32475574.
- He, L., Yan, X., Liang, J., Li, S., He, H., Xiong, Q., Lai, X., Hou, S., & Huang, S. (2018). Comparison of different extraction methods for polysaccharides from *Dendrobium officinale* stem. *Carbohydrate Polymers*, 198, 101-108. <http://dx.doi.org/10.1016/j.carbpol.2018.06.073>. PMID:30092979.
- He, R., Zhao, Y., Zhao, R., & Sun, P. (2015). Antioxidant and antitumor activities in vitro of polysaccharides from *E. sipunculoides*. *International Journal of Biological Macromolecules*, 78, 56-61. <http://dx.doi.org/10.1016/j.ijbiomac.2015.03.030>. PMID:25834926.
- He, Y., Deng, J., Zhao, C., Zhang, J., & Hou, X. (2016). Advances in studies on chemical constituents and pharmacological effects of sugarcane leaves. *Asia-Pacific Traditional Medicine*, 12(08), 49-51. Retrieved from <https://kns.cnki.net/kcms/detail/42.1727.r.20160421.1714.042.html>.
- He, T., Hu, S., Hou, X., & Qin, C. (2016). Effects of sugarcane leaf polysaccharide on electrocardiogram and microangiogenesis of myocardial infarction in rats. *Acta Academiae Medicinae Guangxi*, 33(2), 229-231.
- Heydarian, M., Jooyandeh, H., Nasehi, B., & Noshad, M. (2017). Characterization of Hypericum perforatum polysaccharides with antioxidant and antimicrobial activities: Optimization based statistical modeling. *International Journal of Biological Macromolecules*, 104(Pt A), 287-293. <http://dx.doi.org/10.1016/j.ijbiomac.2017.06.049>. PMID:28602988.
- Hojjati, M., & Beirami-Serizkani, F. (2020). Structural characterization, antioxidant and antibacterial activities of a novel water soluble polysaccharide from *Cordia myxa* fruits. *Journal of Food Measurement and Characterization*, 14(6), 3417-3425. <http://dx.doi.org/10.1007/s11694-020-00586-y>.
- Hou, X. (2014). *Study on chemical constituents and pharmacodynamics of Sugarcane leaves* (Doctoral dissertation). Guangxi Medical University, China.
- Hou, X., Deng, J., Li, A., Wu, Y., Liao, Z., & Guo, Z. (2011). Study on hypoglycemia activity of the different extracts of sugarcane leaves. *Huaxi Yaoxue Zazhi*, 26(05), 451-453.
- Hou, X., Deng, J., Ma, J., Huang, H., & Liao, Z. (2010). Study on in vitro antibacterial activity of sugarcane leaf extract. *Huaxi Yaoxue Zazhi*, 25(02), 161-163.
- Hu, H. B., Liang, H. P., Li, H. M., Yuan, R. N., Sun, J., Zhang, L. L., Han, M. H., & Wu, Y. (2018). Isolation, purification, characterization and antioxidant activity of polysaccharides from the stem barks of *Acanthopanax leucorrhizus*. *Carbohydrate Polymers*, 196, 359-367. <http://dx.doi.org/10.1016/j.carbpol.2018.05.028>. PMID:29891307.
- Hua, D., Zhang, D., Huang, B., Yi, P., & Yan, C. (2014). Structural characterization and DPPH· radical scavenging activity of a polysaccharide from *Guara* fruits. *Carbohydrate Polymers*, 103, 143-147. <http://dx.doi.org/10.1016/j.carbpol.2013.12.009>. PMID:24528712.
- Huang, Y., Li, N., Wan, J.-B., Zhang, D., & Yan, C. (2015). Structural characterization and antioxidant activity of a novel heteropolysaccharide from the submerged fermentation mycelia of *Ganoderma capense*. *Carbohydrate Polymers*, 134, 752-760. <http://dx.doi.org/10.1016/j.carbpol.2015.08.067>. PMID:26428182.
- Hui, H., & Gao, W. (2022). Physicochemical features and antioxidant activity of polysaccharides from *Herba Patriniae* by gradient ethanol precipitation. *Arabian Journal of Chemistry*, 15(5), 103770. <http://dx.doi.org/10.1016/j.arabjc.2022.103770>.
- Jia, Y., Xue, Z., Wang, Y., Lu, Y., Li, R., Li, N., Wang, Q., Zhang, M., & Chen, H. (2021). Chemical structure and inhibition on  $\alpha$ -glucosidase of polysaccharides from corn silk by fractional precipitation. *Carbohydrate Polymers*, 252, 117185. <http://dx.doi.org/10.1016/j.carbpol.2020.117185>. PMID:33183632.

- Jiang, L., Wang, W., Wen, P., Shen, M., Li, H., Ren, Y., Xiao, Y., Song, Q., Chen, Y., Yu, Q., & Xie, J. (2020). Two water-soluble polysaccharides from mung bean skin: physicochemical characterization, antioxidant and antibacterial activities. *Food Hydrocolloids*, 100, 105412. <http://dx.doi.org/10.1016/j.foodhyd.2019.105412>.
- Khaskheli, S. G., Zheng, W., Sheikh, S. A., Khaskheli, A. A., Liu, Y., Soomro, A. H., Feng, X., Sauer, M. B., Wang, Y. F., & Huang, W. (2015). Characterization of Auricularia auricula polysaccharides and its antioxidant properties in fresh and pickled product. *International Journal of Biological Macromolecules*, 81, 387-395. <http://dx.doi.org/10.1016/j.ijbiomac.2015.08.020>. PMID:26277748.
- Khemakhem, I., Abdelhedi, O., Trigui, I., Ayadi, M. A., & Bouaziz, M. (2018). Structural, antioxidant and antibacterial activities of polysaccharides extracted from olive leaves. *International Journal of Biological Macromolecules*, 106, 425-432. <http://dx.doi.org/10.1016/j.ijbiomac.2017.08.037>. PMID:28802847.
- Li, C., Li, X., You, L., Fu, X., & Liu, R. H. (2017a). Fractionation, preliminary structural characterization and bioactivities of polysaccharides from *Sargassum pallidum*. *Carbohydrate Polymers*, 155, 261-270. <http://dx.doi.org/10.1016/j.carbpol.2016.08.075>. PMID:27702511.
- Li, J.-E., Wang, W.-J., Zheng, G.-D., & Li, L.-Y. (2017b). Physicochemical properties and antioxidant activities of polysaccharides from *Gynura procumbens* leaves by fractional precipitation. *International Journal of Biological Macromolecules*, 95, 719-724. <http://dx.doi.org/10.1016/j.ijbiomac.2016.11.113>. PMID:27919812.
- Li, L., Thakur, K., Liao, B.-Y., Zhang, J.-G., & Wei, Z.-J. (2018). Antioxidant and antimicrobial potential of polysaccharides sequentially extracted from *Polygonatum cyrtoneura* Hua. *International Journal of Biological Macromolecules*, 114, 317-323. <http://dx.doi.org/10.1016/j.ijbiomac.2018.03.121>. PMID:29578016.
- Liu, M., Liu, Y., Cao, M.-J., Liu, G.-M., Chen, Q., Sun, L., & Chen, H. (2017). Antibacterial activity and mechanisms of depolymerized fucoidans isolated from *Laminaria japonica*. *Carbohydrate Polymers*, 172, 294-305. <http://dx.doi.org/10.1016/j.carbpol.2017.05.060>. PMID:28606538.
- Liu, Y., & Huang, G. (2019). Extraction and derivatisation of active polysaccharides. *Journal of Enzyme Inhibition and Medicinal Chemistry*, 34(1), 1690-1696. <http://dx.doi.org/10.1080/14756366.2019.1660654>. PMID:31537126.
- Lv, Q.-Q., Cao, J.-J., Liu, R., & Chen, H.-Q. (2021). Structural characterization,  $\alpha$ -amylase and  $\alpha$ -glucosidase inhibitory activities of polysaccharides from wheat bran. *Food Chemistry*, 341(Pt 1), 128218. <http://dx.doi.org/10.1016/j.foodchem.2020.128218>. PMID:33035857.
- Mathlouthi, M., & Koenig, J. L. (1987). Vibrational spectra of carbohydrates. *Advances in Carbohydrate Chemistry and Biochemistry*, 44, 7-89. [https://doi.org/10.1016/S0065-2318\(08\)60077-3](https://doi.org/10.1016/S0065-2318(08)60077-3).
- Mitrović, J., Nikolić, N., Karabegović, I., Lazić, M., Nikolić, L., Savić, S., Pešić, M., Šimurina, O., & Stojanović-Krasić, M. (2022). The effect of thermal processing on the content and antioxidant capacity of free and bound phenolics of cookies enriched by nettle (*Urtica dioica* L.) seed flour and extract. *Food Science and Technology (Campinas)*, 42, 42. <http://dx.doi.org/10.1590/fst.62420>.
- Santhiya, D., Subramanian, S., & Natarajan, K. A. (2002). Surface Chemical Studies on Sphalerite and Galena Using Extracellular Polysaccharides Isolated from *Bacillus polymyxa*. *Journal of Colloid and Interface Science*, 256(2), 237-248. <http://dx.doi.org/10.1006/jcis.2002.8681>. PMID:12573627.
- Shang, H., Cao, Z., Zhang, H., Guo, Y., Zhao, J., & Wu, H. (2021). Physicochemical characterization and in vitro biological activities of polysaccharides from alfalfa (*Medicago sativa* L.) as affected by different drying methods. *Process Biochemistry*, 103, 39-49. <http://dx.doi.org/10.1016/j.procbio.2020.12.011>.
- Shen, S., Cheng, H., Li, X., Li, T., Yuan, M., Zhou, Y., & Ding, C. (2014). Effects of extraction methods on antioxidant activities of polysaccharides from camellia seed cake. *European Food Research and Technology*, 238(6), 1015-1021. <http://dx.doi.org/10.1007/s00217-014-2183-2>.
- Surin, S., You, S., Seesuriyachan, P., Muangrat, R., Wangtueai, S., Jambak, A. R., Phongthai, S., Jantanasakulwong, K., Chaiyaso, T., & Phimolsiripol, Y. (2020). Optimization of ultrasonic-assisted extraction of polysaccharides from purple glutinous rice bran (*Oryza sativa* L.) and their antioxidant activities. *Scientific Reports*, 10(1), 10410. <http://dx.doi.org/10.1038/s41598-020-67266-1>. PMID:32591579.
- Tang, W., Lin, L., Xie, J., Wang, Z., Wang, H., Dong, Y., Shen, M., & Xie, M. (2016). Effect of ultrasonic treatment on the physicochemical properties and antioxidant activities of polysaccharide from *Cyclocarya paliurus*. *Carbohydrate Polymers*, 151, 305-312. <http://dx.doi.org/10.1016/j.carbpol.2016.05.078>. PMID:27474571.
- Tang, L., Luo, X., Wang, M., Wang, Z., Guo, J., Kong, F., & Bi, Y. (2021). Synthesis, characterization, in vitro antioxidant and hypoglycemic activities of selenium nanoparticles decorated with polysaccharides of *Gracilaria lemaneiformis*. *International Journal of Biological Macromolecules*, 193(Pt A), 923-932. <http://dx.doi.org/10.1016/j.ijbiomac.2021.10.189>. PMID:34728301.
- Vicente-García, V., Ríos-Leal, E., Calderón-Domínguez, G., Cañizares-Villanueva, R. O., & Olvera-Ramírez, R. (2004). Detection, isolation, and characterization of exopolysaccharide produced by a strain of *Phormidium 94a* isolated from an arid zone of Mexico. *Biotechnology and Bioengineering*, 85(3), 306-310. <http://dx.doi.org/10.1002/bit.10912>. PMID:14748086.
- Wang, J., Hu, S., Nie, S., Yu, Q., & Xie, M. (2016). Reviews on mechanisms of in vitro antioxidant activity of polysaccharides. *Oxidative Medicine and Cellular Longevity*, 2016, 5692852. <http://dx.doi.org/10.1155/2016/5692852>. PMID:26682009.
- Wang, L., Li, T., Liu, F., Liu, D., Xu, Y., Yang, Y., Zhao, Y., & Wei, H. (2019a). Ultrasonic-assisted enzymatic extraction and characterization of polysaccharides from dandelion (*Taraxacum officinale*) leaves. *International Journal of Biological Macromolecules*, 126, 846-856. <http://dx.doi.org/10.1016/j.ijbiomac.2018.12.232>. PMID:30593815.
- Wang, S., Zhao, L., Li, Q., Liu, C., Han, J., Zhu, L., Zhu, D., He, Y., & Liu, H. (2019b). Rheological properties and chain conformation of soy hull water-soluble polysaccharide fractions obtained by gradient alcohol precipitation. *Food Hydrocolloids*, 91, 34-39. <http://dx.doi.org/10.1016/j.foodhyd.2018.12.054>.
- Wang, K., Guo, J., Cheng, J., Zhao, X., Ma, B., Yang, X., & Shao, H. (2021a). Ultrasound-assisted extraction of polysaccharide from spent *Lentinus edodes* substrate: Process optimization, precipitation, structural characterization and antioxidant activity. *International Journal of Biological Macromolecules*, 191, 1038-1045. <http://dx.doi.org/10.1016/j.ijbiomac.2021.09.174>. PMID:34599988.
- Wang, N., Jia, G., Wang, X., Liu, Y., Li, Z., Bao, H., Guo, Q., Wang, C., & Xiao, D. (2021b). Fractionation, structural characteristics and immunomodulatory activity of polysaccharide fractions from asparagus (*Asparagus officinalis* L.) skin. *Carbohydrate Polymers*, 256, 117514. <http://dx.doi.org/10.1016/j.carbpol.2020.117514>. PMID:33483035.
- Wang, F., Ye, S., Ding, Y., Ma, Z., Zhao, Q., Zang, M., & Li, Y. (2022). Research on structure and antioxidant activity of polysaccharides from *Ginkgo biloba* leaves. *Journal of Molecular Structure*, 1252, 132185. <http://dx.doi.org/10.1016/j.molstruc.2021.132185>.

- Wu, J., Chen, R., Tan, L., Bai, H., Tian, L., Lu, J., Gao, M., Bai, C., Sun, H., & Chi, Y. (2022). Ultrasonic disruption effects on the extraction efficiency, characterization, and bioactivities of polysaccharides from *Panax notoginseng* flower. *Carbohydrate Polymers*, 291, 119535. <http://dx.doi.org/10.1016/j.carbpol.2022.119535>. PMID:35698368.
- Xie, S.-Z., Zhang, W.-J., Liu, W., Bai, J.-B., Xie, S.-L., Wang, T., Xu, G.-B., & Wu, D.-L. (2022). Physicochemical characterization and hypoglycemic potential of a novel polysaccharide from *Polygonatum sibiricum* Red through PI3K/Akt mediated signaling pathway. *Journal of Functional Foods*, 93, 105080. <http://dx.doi.org/10.1016/j.jff.2022.105080>.
- Xu, Y., Guo, Y., Duan, S., Wei, H., Liu, Y., Wang, L., Huo, X., & Yang, Y. (2018). Effects of ultrasound irradiation on the characterization and bioactivities of the polysaccharide from blackcurrant fruits. *Ultrasonics Sonochemistry*, 49, 206-214. <http://dx.doi.org/10.1016/j.ultrsonch.2018.08.005>. PMID:30181026.
- Yalcinkaya, C., Abdalla, H. S., & Bakkalbasi, E. (2022). Bioactive compounds, antioxidant activity, physical and sensory characteristics of Mirra coffee. *Food Science and Technology (Campinas)*, 42, e96221. <http://dx.doi.org/10.1590/fst.96221>.
- Yan, J.-K., Ding, Z.-C., Gao, X., Wang, Y.-Y., Yang, Y., Wu, D., & Zhang, H.-N. (2018). Comparative study of physicochemical properties and bioactivity of *Herichium erinaceus* polysaccharides at different solvent extractions. *Carbohydrate Polymers*, 193, 373-382. <http://dx.doi.org/10.1016/j.carbpol.2018.04.019>. PMID:29773393.
- Yao, W., Liu, M., Chen, X., You, L., Ma, Y., & Hileuskaya, K. (2022). Effects of UV/H<sub>2</sub>O<sub>2</sub> degradation and step gradient ethanol precipitation on *Sargassum fusiforme* polysaccharides: physicochemical characterization and protective effects against intestinal epithelial injury. *Food Research International*, 155, 111093. <http://dx.doi.org/10.1016/j.foodres.2022.111093>. PMID:35400466.
- Yin, C., Fan, X., Fan, Z., Shi, D., & Gao, H. (2018). Optimization of enzymes-microwave-ultrasound assisted extraction of *Lentinus edodes* polysaccharides and determination of its antioxidant activity. *International Journal of Biological Macromolecules*, 111, 446-454. <http://dx.doi.org/10.1016/j.ijbiomac.2018.01.007>. PMID:29309866.
- Yu, L. M., Wu, Y. X., Liu, D. J., Sheng, Z. L., Liu, J. M., Chen, H. G., & Feng, W. H. (2022). The kinetic behavior of antioxidant activity and the stability of aqueous and organic polyphenol extracts from navel orange peel. *Food Science and Technology (Campinas)*, 42, e90621. <http://dx.doi.org/10.1590/fst.90621>.
- Zhang, Z., Lv, G., Pan, H., Pandey, A., He, W., & Fan, L. (2012). Antioxidant and hepatoprotective potential of endo-polysaccharides from *Herichium erinaceus* grown on tofu whey. *International Journal of Biological Macromolecules*, 51(5), 1140-1146. <http://dx.doi.org/10.1016/j.ijbiomac.2012.09.002>. PMID:22982810.
- Zhang, D., Li, S., Xiong, Q., Jiang, C., & Lai, X. (2013). Extraction, characterization and biological activities of polysaccharides from *Amomum villosum*. *Carbohydrate Polymers*, 95(1), 114-122. <http://dx.doi.org/10.1016/j.carbpol.2013.03.015>. PMID:23618247.
- Zhang, D.-Y., Wan, Y., Xu, J.-Y., Wu, G.-H., Li, L., & Yao, X.-H. (2016). Ultrasound extraction of polysaccharides from mulberry leaves and their effect on enhancing antioxidant activity. *Carbohydrate Polymers*, 137, 473-479. <http://dx.doi.org/10.1016/j.carbpol.2015.11.016>. PMID:26686153.
- Zhang, H., Zhao, J., Shang, H., Guo, Y., & Chen, S. (2020a). Extraction, purification, hypoglycemic and antioxidant activities of red clover (*Trifolium pratense* L.) polysaccharides. *International Journal of Biological Macromolecules*, 148, 750-760. <http://dx.doi.org/10.1016/j.ijbiomac.2020.01.194>. PMID:31978472.
- Zhang, K., Ding, Z., Mo, M., Duan, W., Bi, Y., & Kong, F. (2020b). Essential oils from sugarcane molasses: Chemical composition, optimization of microwave-assisted hydrodistillation by response surface methodology and evaluation of its antioxidant and antibacterial activities. *Industrial Crops and Products*, 156, 112875. <http://dx.doi.org/10.1016/j.indcrop.2020.112875>.
- Zhao, C., Li, X., Miao, J., Jing, S., Li, X., Huang, L., & Gao, W. (2017). The effect of different extraction techniques on property and bioactivity of polysaccharides from *Dioscorea hemsleyi*. *International Journal of Biological Macromolecules*, 102, 847-856. <http://dx.doi.org/10.1016/j.ijbiomac.2017.04.031>. PMID:28404222.
- Zhong, H., Su, J., Fang, F., Tan, Y., & Huang, X. (2012). Study on extraction and isolation of sugarcane leaf polysaccharide and its inhibitor effect in vitro. *Journal of Clinical Rational Drug Use*, 5(15), 28-29.
- Zhou, L. B., & Zhang, Q. (2022). Multiple indicators metrological analysis for 5 kinds of tea produced in Yunnan, China. *Food Science and Technology (Campinas)*, 42, e70922. <https://doi.org/10.1590/fst.70922>.
- Zhou, Y., Chen, X., Chen, T., & Chen, X. (2022). A review of the antibacterial activity and mechanisms of plant polysaccharides. *Trends in Food Science & Technology*, 123, 264-280. <http://dx.doi.org/10.1016/j.tifs.2022.03.020>.
- Zhu, R., Zhang, X., Wang, Y., Zhang, L., Zhao, J., Chen, G., Fan, J., Jia, Y., Yan, F., & Ning, C. (2019). Characterization of polysaccharide fractions from fruit of *Actinidia arguta* and assessment of their antioxidant and antiglycated activities. *Carbohydrate Polymers*, 210, 73-84. <http://dx.doi.org/10.1016/j.carbpol.2019.01.037>. PMID:30732783.